Dilatometry of Shape Memory Alloys

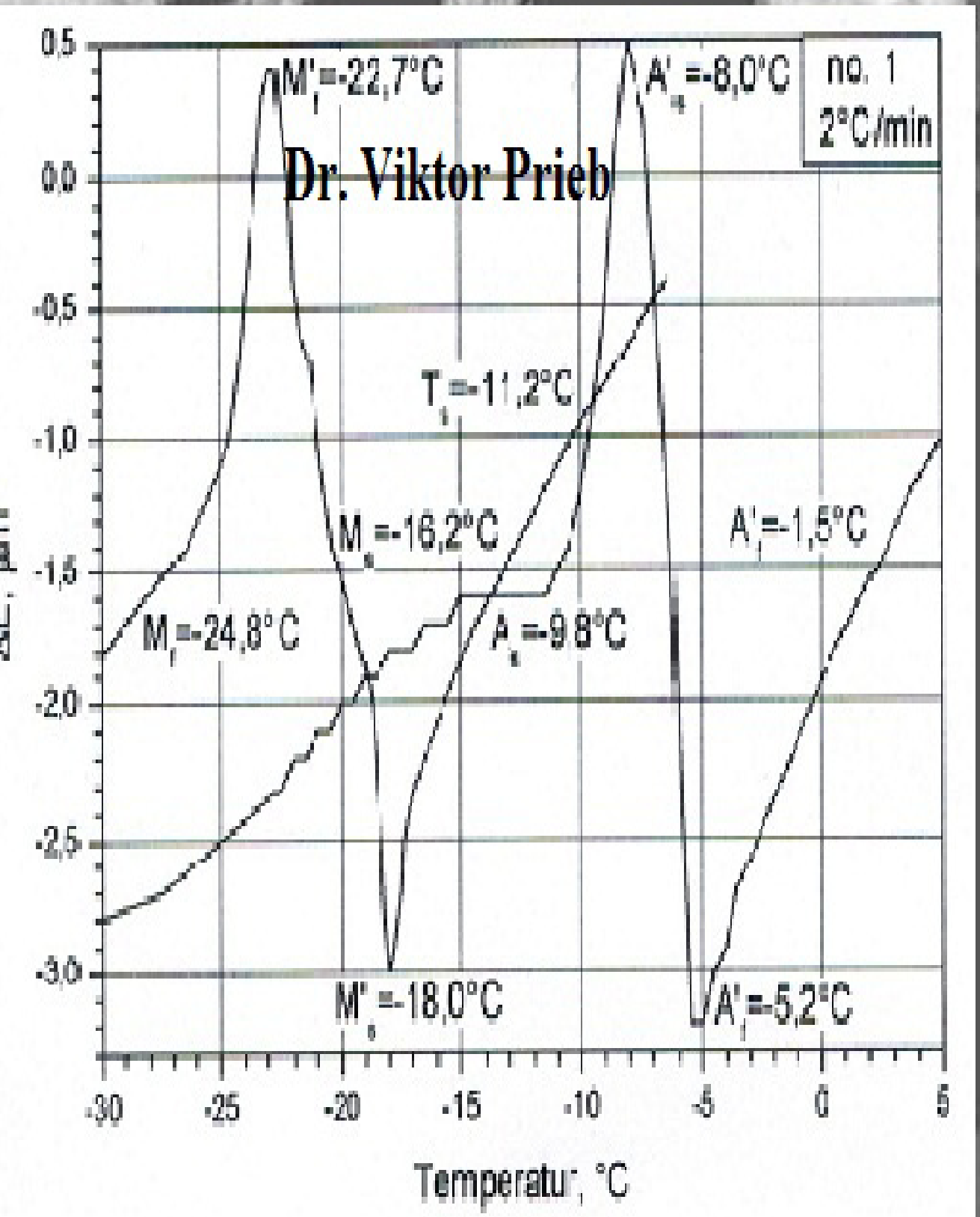

Dilatometry of Shape Memory Alloys

by

Viktor Prieb

„MRS-Bureau Dr. Prieb“ on the TU-Berlin
Berlin, Germany, **20.03.2009**

in cooperation with

Andreas Zilly and Norbert Jost,

“Material Developement and Test Laboratory” of the University Pforzheim

Pforzheim, Germany

Abstract: Three kind of shape memory-alloys (SMA's) – single crystals *Cu-Al-X* (*X*=*Zn, Mn, Ni*), and *MnCu* as well as *TiNi*-polycristals – have been investigated dilatometrically in the temperature interval of martensitic transformations. Three kind of length change (or coefficients of the linear thermal expansion $\alpha = \alpha^{AM/MA}$) have been thereby found in the two phase temperature range: $\alpha = +\alpha^{AM/MA}$, $\alpha = -\alpha^{AM/MA}$ and $\alpha = \pm\alpha^{AM/MA}$, it means sample shorting during the direct transformation and sample lengthening during the reverse transformation and visa versa as well as the both cases during both direct and reverse transformations. The spontaneous sample deformation during the stress-free martensitic transformation differs in different SMA from each other up to one order of magnitude, but lays in all cases in elastic deformation region.

The dilatation effects will be consider as a result of a non-complete accommodation of the martensitic lattice deformation under the elasticity limit (yield) by various accommodation mechanisms. On that basis an accommodation degree as a relation of the measured spontaneous deformation to the martensitic deformation experimental measured by stress-induced transformation is introduced. Its values were calculated for all investigated SMA-samples and lay in an interval from 75% up to 99%.

The thermal expansion of SMA in the temperature interval of martensitic transformations is analysed and discussed on the basis of physical, thermodynamical and crystallographical aspects of martensitic transformations in SMA's.

The width extension of the thermal hysteresis loops depending on the scanning rate is also investigated dilatometrically, and a physical limiting of the work-frequency of SMA-actuators is proved and discussed.

Content:

1. Introduction

The non-elastic effects in shape memory alloys (SMA's) such as the deformation recovery during the heating of a sample pre-formed at the low temperatures (shape memory effect) or during the unloading of a sample pre-loaded at higher temperature (pseudo- or super-elasticity) fascinate the scientists and engineers since their discovering by their possible and partly realised application spectrum as well as even made sure that these alloys have been assigned to intelligent, so-called smart materials.

But in that way SMA's with their sensor-action-functions got a great competition around the other smart-materials such as piezoelectric and magnetostrictive actuator-elements with much higher action frequencies. The shape-memory-actuator lack namely in reaction speed despite much greater deformation and force amplitude in comparing with their electric and magnetic competitors [1]. Nowadays, some much cheaper memory-polymers [2] make a competition to the SMA's, which have an alike great potential of the deformation recovery caused by their molecular long-chain-structure.

The reaction time of SMA-actuators is a sum of cooling and heating time across the characteristic temperature interval of direct and reverse martensitic transformations causing one action-cycle of a SMA-actuators. The action frequency is then the number of complete transformation cycles in one second. This frequency lies below a value of 1 Hz [3].

Nevertheless SMA's are finding at engineers their specific application niches, and they should remain for scientists too an interesting investigation object and not one subordinated to only application aims. Specific martensitic phase transformations, as a basis for the memory properties, are so versatile and deep thorough that they generally contributed with their discovery and research to stimulation of the fundamental research of phase transformations, which were stagnating and came to deadlock after distribution of Nobel Prizes on the superconductivity field, to development of new theories and models and possibly even to new impulses and ideas in the successful development of high temperature superconductors of the most recent time [4, 5].

The speciality of the martensitic phase transformations in SMA's, which provides large reversible deformations at all visualizations of shape memory phenomena, consists of the fact that enormous primary lattice deformation is nearly completely accommodated by the secondary deformation with invariant lattice (twin accommodation as the 1st accommodation mechanism) and by interaction of far growing martensite crystals (the building of complex groups of crystals as the 2nd accommodation mechanism) within elasticity range (without irreversible plastic deformation).

Despite so a fundamental role of accommodation, the accommodation processes and -mechanisms are hardly examined quantitatively, apart from qualitative microstructural observations, although dilatometry presents actually a direct method for the determination of the accommodation degrees by a direct measurement of spontaneous length change of a SMA-sample within the transformation temperature interval.

The caring out of such dilatation measurements on different kinds of SMA-samples with different kinds of martensitic transformations as well as investigation of the temperature dilatation hysteresis loops at different scanning rates were set as aims of this work.

2. Setting of tasks

2.1 Current state of application and research

The mechanical properties of SMA's, which so fascinate inventors, are caused by so-called thermo-elastic martensitic transformations accompanied by a lot of peculiarities and even anomalies of physical characteristics of these metals and/or cause the same, and which could be not less fascinating for researchers. These peculiarities and anomalies would be actually – outside of memory properties – for all kinds of applications, including methodological ones [6, 7], likewise interesting, like their high damping in a broad temperature interval, which are at

least considering as an application in different branches from mechanical engineering to earthquake protection [8, 9].

The anomalies in the temperature dependence of lattice parameters of some memory alloys, which have been determined in X-ray structural investigations and are pointing to macroscopic invar-behaviour (independ-ence of the volume and/or the linear dimensions on the temperature or zero-coefficient of the thermal expansion), are hardly considered concerning this possibility [10] and examined dilatometrically.

For the dilatometry of SMA's it is valid basically nearly as a requirement or a prohibition: these transformations are not to be examined with the help of dilatometry because the crystallographic changes at the martensitic transformations lead to no variation in volume ($V^A \cong V^M$) as well as in coefficients of the thermal volume expansion ($\alpha_V^A \cong \alpha_V^M$), unless a SMA-sample is textured [11], mechanically pre-stressed before the measurements [12] or trained to the two-way memory effect.

But it is forgotten in this way the fact that the same condition ($G^A = G^M$) is valid for the elasticity modulus of the austenite and of the martensite described in the two-phase temperature interval (G^{AM}) according to the additive formula:

$$G^{AM} = G^A \cdot (1 - z) + G^M \cdot z \,. \qquad (2.1),$$

which forbids any changes in the modulus behaviour in this interval.

The anomaly in the temperature behaviour of the elasticity modulus of some SMA's, like its softening during the cooling in pre-martensitic temperature interval, which was found before a long time, is investigated and can cause the elinvar behaviour (elasticity invariantly - independence of the elasticity modulus on the temperature), remains to be excepted from consideration likewise.

Such contradictions are to be attributed to the fact that the investigations of physical properties of SMA's are generally only limited in the most cases to the determination of characteristic trans-formation temperatures including the width of thermal hysteresis and their dependence on dif-ferent metallurgical effects [e.g. 13, 14], which are actually of the interest only for concrete applications. Even these simplest transformation parameters are hardly usable, as long as they are measured, determined and compared at different rates of the temperature change (scanning rates) [15]. This applies even then, if a new SMA is designed, to whose characterization and certification all and above all thermodynamic parameters could be useful, if caloriemetry as a measuring method is already used anyway [16] (for the determination of transformation temperatures at a scanning rate of 20°*C/min*!)

For this simplest task the most expensive and the most complicated equipment - such as a calorimeter e.g. or exceptional too a dilatometer - is frequently used: namely that, what occasionally is present. If however, another one would try to experience from such published "calorimetric" or "dilatometric" investigations somewhat about thermodynamic values like the transformation heat and entropy or over the pure dilatometric parameters like the coefficient of the thermal expansion and its temperature behaviour, this other will be only surprised at the futileness of its attempts and rather comes on the thought that here the nails were hit by a computer instead by a simple hammer.

It were enough to use as "the hammer" for the measurements of transformation temperatures – and it have also since a long time been used [13] - a tinkered device for the four-pole-measurements of the electrical resistance with cooling-heating possibilities. This measuring method yields sure (with consideration of the previous remark about the scanning rate) results about the characteristic transformation temperatures, because the electrical resistance of the high-symmetrical austenite is never equal to that of the low-symmetrical martensite, and the change of the electrical resistance of a SMA-sample described according to additive formula similar (2.1) mostly is very clear and measurable.

However, even this simple method offers also excellent possibilities to investigate at least indirectly, qualitatively the changes in the electron structure before and during the transformation. Only the fact arouses the curiosity of scarcely someone from scientists, that the electrical resistance of metallic *Cu*-basis SMA's is changing "normal" (increases at the transition to a low-symmetric phase) during the direct transformation and behaves complete "abnormally" in binary inter-metallic *NiTi*-SMA's, where interaction between phonons and electrons (between the borders of the Brillouin-zone and the Fermie-surface) plays an important role: It is remaining constant in a broad pre-martensitic temperature interval, increases then at the transition to R-phase with the symmetry like that of *B2*-phase and decreases finally in contrast to *Cu*-basis alloys in the low-symmetrical *B19'*-phase with another temperature coefficients than that of the austenite. The electrical resistance of alloyed $Ti_{50}Ni_{40}X_{10}$ (*X=Cu, Pd, Pt, Au*) SMA's is increasing during the transformation again "normal", although the symmetry of the *B19*-phase is significant higher than those of the monoclinic distorted *B19'*-phase. Such anomalies can in no way be described and explained so simply as by the additives formula (2.1).

It is mostly the only one disadvantage of these "primitive" and frequently "tinkered" measuring devices to ensure a regular, well-balanced and pre-programmed cooling and heating rate. But investigators also too often neglect to examine and to take into consideration at the using of complex measuring systems with integrated regulating equipment, the influences on the results of measurement of some not only technical, like inertia of the heating-cooling system, but also pure physical conditions.

It concerns, for example, the already mentioned scanning rate at stress-free thermal measurements as well as iso-stress conditions (either a sample is loaded statically by one hanging weight or held at one "constant" load dynamically by a computer-controlled high-speed engine [17]), and/or the velocity of the mechanical loading and unloading at the isothermal stress-strain measurements as well as the real environment medium (air, water, oil etc.), which ensure the iso-thermal conditions. There are already enough experimental proofs that all these circumstances influence both the width and the form of the both thermal and mechanical hysteresis loops substantially [15].

If sometimes - although rarely - a complex investigation with a good theoretical draft and task is nevertheless undertaken with the help of complex measuring systems such as a calorimeter, the results in some cases are more than curious and show only, that the researcher had too much confidence in this measuring method, perhaps directly due to its modernity and complexity, without the specificities of both transformation and methodical conditioned backgrounds and artefacts to understand and to examine.

In this way the partial transformation cycles were in a calorimeter accomplished to prove the presence or absence of shear tensor components of the internal stresses stored in the accommodated martensite of the transforming sample. They had to cause the shift of the M_S-temperature in partial cycles realized by interruption of the reverse transformation and following cooling. Thus, the accommodation degree of the martensitic lattice deformation could be determined [18].

The results showed not only no shift of the M_S-temperature, but also no heat flow change at the direct transformation in the sample after the everyone interrupting of the reverse transformation at different, each time smaller becoming phase fractions of the austenite. The author interpreted the first of both as a proof of the absence of the internal shear stresses in the two-phase sample, what was forecasted by him theoretically, but he had not even think to interpret the second of both. The theoretician did not see simply away his discovery breaking spell and everything else: eternal looked for - the 2nd rule of thermodynamics to the defiance - Perpetuum Mobile!

Because the heat absorbed from the environment during the reverse transformation may never be smaller in an thermal insulated thermodynamic system, according to the 2nd rule of thermodynamics, than the heat spent to the environment during the reverse transformation. Since this heat is proportional transformed phase fraction, as it is strongly assumed in the thermoelasticity model, the heat absorbed in partial cycles during each time smaller becoming phase fraction of the transformed austenite was more and more reduced under the value of the

heat spent during the direct transformation, where it was remaining constant in every cycle. Thus, the energy winning forbidden according to the 2nd rule took place more and more.

Such experimental nonsense results, which do not accord with all existing knowledge, but accord – even though by a manipulation like it in [19] – with a new model or theory developed by mathematician as an experiment draft and the research task, are unfortunately caused not only by the confidence of an experimenter on the measuring systems or by the unawareness of the mathematician in basic properties of SMA's, but also by the bad states in scientific relationships between often foreign, easily blackmailed experimenter-graduate-students [19] and the ambitious native theoretician-professors.

2.2 To be clarified questions

It was shown in earlier investigation [15] that the width of thermal transformation hysteresis increases with the increasing of the scanning rate as a result of shifting of all characteristic transformation temperatures (excepting the equilibrium temperature). This means that the martensitic transformation in shape memory alloys cannot be accelerated by the increasing of the cooling-heating-rate or only in small measure. The highest limit value of the action frequency calculated from measured results for all investigated SMA's lays far under 1 cycles per second (far under 1 *Hz*), whereas this frequency is imagined over 100 *kHz* in some theoretical simplest computations in the assumption the transformation temperature interval remains constant by unlimited increasing of the scanning rate.

The far under 1 *Hz* laying frequency limiting exists due to the latent transformation heat, which is to be conducted away during the direct transformation and due to heat which is to be supplied during the reverse transformation, but cannot be transferred due to the approximation of the heat transfer more and more to the adiabatic conditions at the increasing scanning rate. It could finally bring a SMA-actuator with work frequencies in a *kHz*-range fast to the glowing, even through the transformation ignores this physical limitation.

On the other hand, this far under 1 *Hz*-limit was found in calorimetric measurements – in the direct heat flow measurements. Thus, it nevertheless remains doubt, whether the measured increasing of the hysteresis width could be caused by the time-delayed propagation of the heat front in SMA-samples, while the heat source has been already switched off – it means the transformation would actually be long to end. It is strictly assumed for the athermic martensitic transformations according to the Kurdjumov thermo-elasticity model, that the transformation continues only by changing of the temperature and remains to stay at the temperature standing.

The calorimetric investigations of partial martensitic transformations in SMA's with narrow thermal hystereses [20] has been showed however – exactly the same as the results with the injury of the 2nd rule of thermodynamics [18] described above – that the direct transformation is complete in accordance with heat content only because the reverse transformation had also completely run off, despite its interruption in partial cycles at the phase fractions values of austenite from less than 100% up to hardly over 50% in accordance with the calorimetric transformation curve – thus on the right shoulder of the heat flow peak.

This doubt can be eliminated only by measurements of the changes of physical characteristics connected directly with the martensitic transformation and not of heat traces of the transformation as a function of scanning rate.

In this work comprehensive results of dilatation measurements on different SMA's are presented, and the connection between dilatometric and some physical characteristics as well as repeatedly the physical limiting of the working frequency of SMA-actuators are discussed.

3. Martensitic phase transformation in shape memory alloys

3.1 Historical consideration

Intensive basic research of martensitic transformations, which cause reversible deformation of a metal pieces (shape memory effects), begun after the discovery by Buehler [21] these ef-

fects (two lines of plastic flow in the stress-strain-diagrams) at the new developed equi-atomic inter-metallic *NiTi* compound in the year 1962 in the "US Naval Ordnance Laboratory" (the abbreviation "NOL" has given the original name to the new alloy „Nitinol ").

The fundamental investigations of SMA are stagnating since ninetieth years of the last century and degraded not only by scientists, but in a large measure by the research promoting government financial programs to purely application specific ones and replaced through computer calculation modeling by laymen and by far from fundamental knowledge of SMA staying scientists. Nowadays, this state of research cannot change so much as the after scarcely 40 years renewed discovery of two lines of plastic flow in the stress-strain-diagrams of *NiTi* [22] and the renewed inspiration of scientists connected with that.

The terms and definitions for the martensitic phase transformation in SMA's fixed and with the time established from the beginning are only partially correct and sometimes even irritating and misleading. They are only from crystallographic point of view martensitic transformations in the traditional sense, which happen diffusionless – by cooperative shift of certain atomic plans in certain crystallographic directions. This determines also the presence of strict orientation relationships between the crystal lattices of the austenite and the martensite as well as the appearance of a surface relief.

The definition "thermo-elastic" for kinetics of these specific transformations, introduced by Kurdjumov, actually irritates therefore that this term was already established in former times within another research field and for another phenomenon. The well-meant similarity of the near to linear size and/or of phase fraction change of the martensite crystals with the temperature change to the linear and reversible deformation under external stress in the elasticity range remains only a superficial one, because these changes in the martensitic phase are in principle irreversible and in this meaning not elastic, accompanying by energy dissipation and exhibit a hysteresis between athermic, but in some cases also isothermic [17] trajectories of the direct and reverse martensitic transformations.

The transformations in SMA's are founding rather their own special class of phase transitions differ despite the existing of the hysteresis from the traditional martensitic transformation in ferrous alloys and steels, which "explode" with the speed of sound in metals and at which the transformation hysteresis is broader from one up to two order of magnitude. These transformations in most SMA's are similar the symmetry changes of the crystal lattice accompanying the transitions of the 2nd order in ferromagnetic and anti-ferromagnetic as well as in segneto-electric materials and superconductors, which are described by Landau-Ginsburg theory. One of them is investigated also in this work on the example of the martensitic transformation accompanying the anti-ferromagnetic ordering in a *Mn-Cu*-SMA.

In this sense the martensitic transformations in SMA's can be designated as the phase transitions of close to the 2nd order ones or as the transitions of the weak 1st order, how this is already introduced with regard to the $B2 \Leftrightarrow R$ -transformations in *TiNi*-SMA's with a very narrow hysteresis (2-3°C). This designation means that the martensitic transformations in the most SMA's exhibit the transition characteristics of both the 1st and the 2nd order.

3.2 Classical consideration – the equilibrium thermodynamics

As the transitions of the 1st order are defined in thermodynamics those, at which a jump of the first derivatives of thermodynamic potentials takes place at the transition temperature. The first derivatives of e.g. the free enthalpy (Φ called also Gibbs' potential):

$$d\Phi = -SdT + Vdp\,, \tag{3.1}$$

are the entropy *(S)* and the volume *(V)* and/or the lattice deformation (ε) during the loading by uni-axial external mechanical stress (σ):

$$S(T,p) = -\frac{\partial \Phi}{\partial T}\,, \quad V(T,p) = \frac{\partial \Phi}{\partial p} \text{ and/or. } \varepsilon(T,\sigma) = \frac{\partial \Phi}{\partial \sigma}\,. \tag{3. 2}$$

In the same terms for the lattice deformation and external stress the equilibrium trajectory $T_0(\sigma)$ can be computed from eq. (3.1) at the temperature $T = T_0$:

$$d\Phi = -\Delta S^{AM} dT + \Delta\varepsilon^{AM} d\sigma = 0, \tag{3.3}$$

$$\frac{dT_0}{d\sigma} = \frac{\varepsilon^M}{\Delta S^{AM}}, \tag{3.4}$$

whereby $\Delta S^{AM} = S^M - S^A$, $\Delta\varepsilon^{AM} = \varepsilon^M - \varepsilon^A \equiv \varepsilon^M$ are the entropy and lattice deformation differences between the austenite (index *A*) and the martensite (index *M*) at the direct transformation (index *AM*). The representational form (3.4) is well-known as modified Clapeyron- Clausius' relation.

Thus, at the transitions of the 1st order between the phases *A* and *M* it is valid the following:

$$S^M \neq S^A \text{ and } V^M \neq V^A \text{ or } \varepsilon^M \neq \varepsilon^A, \tag{3.5}$$

what on the other hand means:

$$Q = T \cdot (S^M - S^A) := T\Delta S^{AM} \neq 0 \text{ and } W = p \cdot \Delta V^{AM} \neq 0 \tag{3.6}$$

The latest means that the transitions 1st order are accompanying by the spending and adsorption of the transition heat (Q) – so-called latent transformation heat – or by the performing of the mechanical work (*W*) on the environment and on the system.

At the transitions of the 2nd order the entropy and the volume or the lattice deformation of both phases or a one for the system selected order parameter η are in the transition point each other equal:

$$S^M = S^A \text{ and } V^M = V^A \text{ and/or } \varepsilon^M = \varepsilon^A. \tag{3.7}$$

For these reasons the transitions of the 2nd order are called "continuous transitions".

The second derivatives of thermodynamic potentials:

$$\left(\frac{\partial^2\Phi}{\partial T^2}\right)_p = -\frac{c_p}{T} \text{ and } \left(\frac{\partial^2\Phi}{\partial p^2}\right)_T = -V \cdot \kappa \tag{3.8}$$

as well as the mixed derivatives:

$$\left(\frac{\partial^2\Phi}{\partial T\partial p}\right)_p = -\left(\frac{\partial S}{\partial p}\right)_T \text{ and } \left(\frac{\partial^2\Phi}{\partial p\partial T}\right)_T = \left(\frac{\partial V}{\partial T}\right)_p = V \cdot \alpha_V \tag{3.9}$$

exhibit the finite or infinite jumps in the transition point, whereby c_p is the isobar thermal capacity, κ – compressibility and α_V – coefficient of the thermal volume expansion.

3.3 Connections between dilatometeric, calorimetric and mechanical parameters

3.3.1 Entropy and the thermal expansion

Because the mixed derivatives in equation (3.9) are identical, an important connection between the coefficient of the thermal volume expansion and the pressure dependence of the entropy arises:

$$\left(\frac{\partial S}{\partial p}\right)_T = -V \cdot \alpha_V. \tag{3.10}$$

For anisotropic solids, to which first of all belong low-symmetrical crystals, linear characteristics of the compressibility and the thermal expansion should be introduced, which are valid in different axial directions of the crystal lattice. The variation in volume depends on a temperature or a pressure change is represented by a dimensionless strain:

$$\varepsilon(T,p) := \ln\left(\frac{V}{V_0}\right) = \ln\left(\frac{L_x}{L_0}\right) + \ln\left(\frac{L_y}{L_0}\right) + \ln\left(\frac{L_z}{L_0}\right) \qquad (3.11),$$

whereby L_i ($i = x, y, z$) are the size of the crystal in direction of three lattice axes ($V = \prod_i L_i$).

If an uni-axial mechanical stress σ_i instead of a hydrostatic pressure affects on a crystal in any direction j ($j \neq i$), the reaction of the crystal to this effect would be described by one the compressibility similar value s_{ij} in its tensor form:

$$s_{ij} = \left(\frac{\partial \varepsilon_i}{\partial \sigma_j}\right)_{T,\sigma'} \qquad (3.12)$$

It is valid at small stresses (within the elastic range):

$$\vec{\varepsilon} = \hat{s} \cdot \vec{\sigma} \text{ or } \vec{\sigma} = \hat{s}^{-1} \cdot \vec{\varepsilon} := \hat{c} \cdot \vec{\varepsilon}, \qquad (3.13)$$

whereby $\hat{c} := \hat{s}^{-1}$ (the both are tensors 2nd stage) is the elasticity tensor. The equation (3.10) in this consideration will be rewritten as stress dependencies of the entropy in connection with the coefficients of the linear thermal expansion:

$$\alpha_i = \frac{1}{L_i} \cdot \left(\frac{\partial L_i}{\partial T}\right)_{\sigma} \qquad (3.14),$$

$$\alpha_i = \frac{1}{\varepsilon} \cdot \left(\frac{\partial S}{\partial \sigma_i}\right)_{T,\sigma'} \qquad (3.15)$$

whereby σ' designates all different except σ_i possible components of the mechanical stress in different directions.

3.3.2 Elastic modulus and the thermal expansion

Elastic characteristics of solids reflect the interaction of atoms which built the crystal lattice of the corresponding solids. This interaction represents by means of a model potential in the such form, which at the nearest surroundings corresponds to the experimentally measured values and in the best way describes the solid and its behaviour. At most one of the form of model potential which is used in the simulations is the following one:

$$U(r) = \frac{a}{r^m} - \frac{b}{r^n}, \quad m > n; \quad a, b > 0 \qquad (3.16)$$

(at $m = 12, \quad n = 6$ it is known as Lenard-Jones' potential).

From the equilibrium condition at $r = r_0$, where the potential (3.16) exhibits a minimum:

$$U'(r_0) = -\frac{am}{r_0^{m-1}} + \frac{bn}{r_0^{n-1}} = 0 \qquad (3.17)$$

we obtain the value for $r_0 = \left(\frac{ma}{nb}\right)^{\frac{1}{m-n}}$, so that we can now represent equilibrium values of the potential and its all derivatives at $r = r_0$:

$$U(r_0)=\frac{a(1-\frac{m}{n})}{r_0^m}<0, \tag{3.18}$$

$$U^{(k)}(r_0)=\frac{(-1)^k}{r_0^k}\cdot\frac{mn}{n-m}\left[\prod_{i=0}^{k-1}(m+i)-\prod_{i=0}^{k-1}(n+i)\right]U(r_0)=(-1)^k\cdot K(k)\cdot\frac{U(r_0)}{r_0^k}. \tag{3.19}$$

where $K(k)$ is a number combination constant for every derivative.

The model potential and its derivatives in the vicinity of the r_0 may be presented through only its equilibrium value $U(r_0)$ by means of Taylor expansion as follows:

$$\begin{aligned}
U(r)&=U(r_0)+\frac{1}{2}U''(r_0)\cdot(r-r_0)^2+\frac{1}{6}U'''(r_0)\cdot(r-r_0)^3+...\approx U(r_0)\\
U'(r)&=U''(r_0)\cdot(r-r_0)+\frac{1}{2}U'''(r_0)\cdot(r-r_0)^2+..\approx U''(r_0)\cdot(r-r_0)\\
U''(r)&=U''(r_0)+U'''(r_0)\cdot(r-r_0)+\frac{1}{2}U''''(r_0)\cdot(r-r_0)^2...\approx U''(r_0)+U'''(r_0)\cdot(r-r_0)
\end{aligned}. \tag{3.20}$$

The potential fast rises to the infinity at $r<r_0$ with the tending of the atoms due to the repulsive force between the atoms. At $r>r_0$ the attraction force between the atoms outweighs, which fast weakens with the distance enlargement between the atoms, so that the potential goes against zero at $r>>r_0$. The potential describes the linear elastic deformation in the vicinity of the r_0, where its form is still close to the parabolic-symmetrical, whereas its asymmetry (anharmonicity) is the cause for the thermal expansion. This allows to bring the elastic characteristics in connection with those of the thermal expansion.

The elastic shear modulus (*G*) can be determined from the Hooke's law: $\sigma=G\cdot\varepsilon,\ G=\frac{\sigma}{\varepsilon}$ and from the form (3.16) of the potential, if the deformation ε is represented through the interatomic distances before (r_0) and after (r) the loading by external stress (σ) as the force $F=-gradU(r)=-U'(r)$ affecting on the attack square $A=r_0^2$:

$$\varepsilon=\frac{r-r_0}{r_0},\qquad \sigma=\frac{F}{A}=\frac{-U'(r)}{r_0^2},\qquad G=\frac{1}{r-r_0}\cdot\frac{-U'(r)}{r_0} \tag{3.21}$$

From (3.21) with the consideration (3.20) we obtain the proportionality to the second derivative of the potential for the equilibrium elastic shear modulus G_0 at the absolute zero temperature (without thermal oscillations $r=r_0$) and for the elastic modulus G at a temperature *T* correspondently:

$$G_0=G(r_0)=\frac{-U''(r_0)}{r_0}\ \text{and}\ G=G(r)=\frac{-U''(r)}{r_0}. \tag{3.22}$$

So we can calculate now with the help of the expression for the second derivative of the model potential (3.20) and the rewriting of the equation (3.19) for the second and for the third derivations the change of the elastic modulus at the temperature rising from zero to *T* and its connection with the thermal expansion:

$$\frac{G-G_0}{G_0}=\frac{U'''(r_0)}{U''(r_0)}(r-r_0)=-\frac{K(k=3)}{K(k=2)}\cdot\frac{(r-r_0)}{r_0}=-k_1\alpha T \tag{3.23}$$

where $k_1 = \frac{K(k=3)}{K(k=2)}$.

If we differentiate the equation (3.23) with respect to the temperature, we will reveal the connection between the temperature coefficient of the elastic modulus $\frac{dG}{dT}$ and the coefficients of the linear thermal expansion α:

$$\alpha = -\frac{k_1^{-1}}{G_0} \cdot \frac{dG}{dT}, \tag{3.24}$$

The coefficient of the thermal expansion is, thus, a fundamental characteristic of solids and its behaviour at the affecting of external parameters (temperature, stress etc.) allows to make certain conclusions about other internal parameters and it can be predicted by the analysis of other well-known transformation characteristics.

4. Experimental

4.1 Kind of materials and transformations

As investigation objects were chosen the SMA's (Table 1), which present the most well-known and practically applicable alloys with memory properties and with the most well-known, thermodynamic, crystallographic and physical various martensitic transformations.

The martensitic transformations in *Cu*-basis SMA's lead to the building of low-symmetric, long-periodic martensitic structures (*9R, 2H*) from the high-symmetric austenite ordered to the *B2*- or sometimes DO_3-strukture type. They all show similar values of the specific (related to mass unit) latent transformation heat ($q^{AM/MA}$) and the specific transformation entropy ($\Delta s^{AM/MA}$), but very different hysteresis widths (ΔT) and correspondingly very different values of the dissipated energy $w_D^T = \Delta s \cdot \Delta T$ [23] (Table 2).

The well-known transformation of the *B2*-austenite to the martensite ordered to the *B19*-strukture type with monoclinic distortion ($B2 \leftrightarrow B19'$) takes place in *NiTi* alloys [24]. The rhombohedric distortion of the cubic crystal lattice $B2 \leftrightarrow R$ – as a transformation closed to the transitions of the 2nd order with a small hysteresis is separated in sample 7 by a bit higher *Ni*-content from the $B2 \leftrightarrow B19'$-transformation. The maximal martensitic deformation reaches 2% at the $B2 \leftrightarrow R$-transition, and 5% at the $B2 \leftrightarrow B19'$-transition in poly-crystals *NiTi*. Both *Cu*-basis and *NiTi* alloys exhibit softening of the elastic modulus in pre-martensitic temperature range.

Table 4.1 Compositions (at%), crystal states, types of transformation, orientations of the sample longitudinal axis and the output lengths of the examined samples

no.	Crystal state	transformation type	*Cu*	*Al*	*Zn*	*Mn*	*Ni*	*Ti*	$[hkl]_A$	L_0, *mm*
1	single	$B2 \leftrightarrow 9R\ (\beta_1 \rightarrow \beta'_1)$	68.8	15.2	16.0	---	---	---	100	9,6
2	single *	$B2 \leftrightarrow 9R\ (\beta_1 \rightarrow \beta'_1)$	68.6	20.7	---	10.7	---	---	110	9,5
3	single	$B2 \leftrightarrow 2H\ (\beta_1 \rightarrow \gamma'_1)$	70.7	24.9	---	---	4.4	---	110	9,6
4	single **	$B2 \leftrightarrow 2H\ (\beta_1 \rightarrow \gamma'_1)$	70.6	24.7	---	---	4.7	---	110	14,3
5	single	$fzk \leftrightarrow fzt$	15.9	---	---	84.1	---	---	100	9,6
6	poly	$B2 \leftrightarrow B19'$	---	---	---	---	49.8	50.2	---	9,6
7	poly	$B2 \leftrightarrow \frac{B19'}{R}$	---	---	---	---	50.5	49.5	---	13,0

** Single crystal with a developed block structure*
***Chochralsky's growing method*

A tetragonal distortion (with axis ratio $c/a<1$ [25]) of the face-centred cubic crystal lattice of the austenite ($fzk \rightarrow fzt$) in *Mn-Cu*-alloy (sample 5) is also a martensitic transformation close to the transitions of the 2nd order, which is connected with the anti-ferromagnetic ordering of the paramagnetic austenite and takes place at Neel-temperature T_N ($T_t = T_N$). The shape and slope of the hysteresis loop are thereby determined not only by the growth of the phase fraction of the fzt-martensite, but also by the temperature dependence (Brilluoin's function) of the axis ratio and/or the parameter $\eta = (1 - c/a)$ in the fzt-martensite as the order parameter. The maximal reversible deformation (η) reaches about 0,02 like that at the $B2 \leftrightarrow R$ - transformation in *NiTi*.

Thus, different martensitic transformations in a temperature range from - 100°C (173 K) to +200°C (473 K) have been covered in this investigation.

4.2 Sample preparation, thermal treatment, transformation temperatures

All alloys (Table 1) have been melted from components with the purity 99.99%. The compositions have been calculated by the output component ratio and controlled by REM- analysis.

Single crystals of the *Cu*-basis (1 - 3) as well as *Mn-Cu* (5) alloys have been grown according to Bridgement's method, while the *Cu-Al-Ni* alloy (4) – according to Chochralsky's method. The *NiTi* alloys (6, 7) were poly-crystals, whereby samples 6 have been cut out from a rolled plates with a thick of 1 *mm* and samples 7 – from the pulled wire with a diameter of 1,5 *mm*.

The following for this SMA's well-known standard heat treatments have been used:

1. *for Cu basis alloys::* annealing at 850°C K for 0,2 h and quenching into oil at 150°C + tempering at this temperature for 0,5 h and quenching into water at the room temperature;
2. *for Mn-Cu alloy:* annealing at 850°C for 0,5 *h* and quenching into cold water + aging at 450°C for 1*h* then air cooling;
3. *for NiTi-alloys:* annealing at 850°C for 0,5 *h* and quenching into cold water.

The characteristic temperatures and thermodynamic parameters of all martensitic transformations were calorimetric measured and then calculated [23].

Table 4.2. Characteristic transformation temperatures (°C,) and thermodynamic parameters of the samples from the Table 4.1 .

no.	M_s	M_f	A_s	A_f	ΔT	q^{AM}/q^{MA}, J/kg	$\Delta s, \frac{J}{kg \cdot K}$	$w_D^T, \frac{J}{kg}$
1	-16.2	-24.8	-9,8	-1,5	18,3	5660/-6300	23,0	421

2	32.0	21.6	44.0	49.8	20,1	6600/ -6800	22.0	442
3	18.2/-12.2	6,0/-29.0	- 7.0/26.0	10,0/36.0	18,9/22,1	7200/ -7600	22,1	477
4	-15,7	-20,5	-12,0	- 9,3	7,0	7400/ -8500	20.7	145
5	162,4	153,0	156,0	167,2	3,9	2600/ -2600	5.6	22
6	64.0	56.0	96,0	104,0	40,0	27700/-27900	81.3	3252
7	-4,0 T_R=49	-19,0	19,2	37,0	39,6 3,5	27700/-27900 7450/ -7860	81.3 24,0	3220 80

The samples for calorie and dilatation measurements have been cut out of the same crystals and semi-finished materials. All dilatometric samples got flat polished endings.

4.3 Investigation methods

The structural and orientation investigations of single crystals were carried out in an transmission electron microscope (TEM) JEOL-200C [26], the composition analysis – in a scanning electron microscope (REM).

The latent transformation heat and the characteristic transformation temperatures were measured in a differential scanning calorimeter DSC-7 “PERKIN ELMER" PC-series with a full-computerized experiment control and acquisition of calorimetric data. The converting of calorimetric curves into loops of thermal hysteresis was done with a help of the program "Partial Area", which calculates the transformation degrees as the phase fraction (*z*) at each forgiven temperature in the two-phase temperature range. This methodology including the determination of transformation temperatures and calculation of the equilibrium temperature had been described in detail in [23].

Changes of the sample length in temperature ranges of - 100°C to 300°C at different and holding during of each measurement the cooling and heating rate constantly was measured in a NETZSCH dilatometer with the using of a low-temperature measuring element, whereby a horizontal pipe-furnace, pushed over it, with a coat cooling by liquid nitrogen, makes possible the change of temperature for the whole measuring instrument with the sample holder. The thermocouple contacted the surface of the measured sample, whereby the heat contact was made sure by a thermal paste.

The coefficients of the linear thermal expansion were calculated with the help of the integrated software “Thermal Analysis”. All diagrams of experimental results were drawn with the computer programme “ORIGIN 6.0”.

5 Experimental results

5.1 Dilatometric and calorimetric hysteresis loops and parameters

5.1.1 Cu-basis shape memory alloys

Dilatometric results for *Cu*-basis SMA’s were recorded only on single crystals with two different orientations of the longitudinal axis (Table 4.1) (Fig. 5.1 - 5,4). As it can be seen from these graphics, the measured and calculated parameters, such as the length change and the coefficient of the linear thermal expansion, differ not only on their value, but also on their signs. The values determined from these graphics are collected in Table 5.1 for all examined SMA’s.

In the columns of the table both absolute dilatation $\Delta L = L - L_0$ in *μm*, and relative dilatation of samples as deformation $\varepsilon_d = \frac{\Delta L}{L_0} \cdot 100\%$ are indicated, as well as the coefficients of the linear thermal expansion in the pure austenite (α^A) and martensite phases (α^M) and in two-phase temperature ranges during the direct (α^{AM}) and reverse transformations (α^{MA}).

The latter values reflects rather kinetic characteristics of the transformation, as the physical thermal expansion of two-phase mixtures. Different values of α^{AM} and α^{MA} refer to an

asymmetry of the hysteresis loop, so that a quantitative dimensionless measure of the hysteresis loops asymmetry can be introduced:

$$A_H = \frac{\alpha^{AM}}{\alpha^{MA}} \tag{5.1}$$

Asymmetry values calculated in this way are also introduced to the table and show that only the hysteresis loop of sample 3 is symmetrical ($A_H = 1$). The most other hysteresis loops are asymmetrical, whereby both cases are present: $A_H < 1$ (samples 1, 2, 7) - the direct transformation is slower, than the reverse transformation and $A_H > 1$ (samples 4, 5, 6) – visa versa. We speak about transformation or deformation velocity because:

$$\frac{\alpha^{AM}}{\alpha^{MA}} = \frac{1}{L_0}\cdot\frac{d\Delta L^{AM}}{dT} \Big/ \frac{1}{L_0}\cdot\frac{d\Delta L^{MA}}{dT} = \frac{d\varepsilon^{AM}}{r_{sc}\cdot dt} \Big/ \frac{d\varepsilon^{MA}}{r_{sc}\cdot dt} = \frac{\dot{\varepsilon}^{AM}}{\dot{\varepsilon}^{MA}}, \tag{5.2}$$

whereby r_{sc} is the constant scanning rates pre-programmed for each measurement and

$$\dot{\varepsilon}^{AM/MA} \equiv \frac{d\varepsilon}{dt} = \frac{1}{L_0}\cdot\frac{d\Delta L^{AM/MA}}{dt} \tag{5.3}$$

is namely the velocity of the length change during the transformation with a constant scanning rate. At $A_H = 1$ the hysteresis loop is ideally symmetrical. The sign refers to whether shortening ($-\Delta L,\ +\alpha$) or extension ($+\Delta L,\ -\alpha$) of the sample tooks place during the transformation.

Table 5.1 Length change (*μm*), deformation (*%*) and the coefficient of the linear thermal expansion (K^{-1}) in austenitic, martensitic and two-phase states within the transition temperature interval

Sample-no.	ΔL	ε_d	$\alpha^A \cdot 10^6$	$\alpha^{AM} \cdot 10^6$	$\alpha^M \cdot 10^6$	$\alpha^{MA} \cdot 10^6$	A_H	k_a
1: γ	+3,7	+0,04	18,0	-170	7,0	-240	0,7	0,994
β'_1	-1,7	-0,03		+130		+100	1,3	0,996
2	-120,0	-1,26	24,0	1490	24,0	2950	0,5	0,750
3	+60,0	+0,63	18,0	-380	0,0	-380	1,0	0,840
4	+22,0	+0,15	5,0	-1180	13,0	-1050	1,1	0,960
5	-48,0	-0,50	45.0	510	40,0	430	1,2	0,750
6	-15,0	-0,16	8,0	210	8,0	190	1,1	0,970
7: B19'	+2,4	+0,02	25,0	-22	12,0	-30	0,7	0,997
R	+4,0	+0,03		--	10,0	-210	--	0,990

The unusual dilatation behaviour of the single crystal sample no. 1 in the transformation temperatur interval (Fig. 5.1 a) is very interesting. The direct transformation begins with increasing of the normal shortening of the sample during the cooling. After the reaching of the temperature interval of the linear growth of the martensitic phase ($\frac{dz}{dT} = const$, Fig. 5,1 c) the fast extension of the sample starts then suddenly. On the end of the temperature interval of the linear growth the shortening of the sample sets jump like repeatedly.

On the first view a such behaviour appears to correspond to the transitions of the 2nd order with a finite jump of the second derivatives of the thermodynamic potential (3.8) and (3.9). However, calorimetric curves show typical for transformations of the 1st order exothermal (direct transformation) and endothermal (reverse transformation) monotonous peaks.

Such jumps of the length changes would be possible by the interchange of two different martensitic transformations $\beta_1 \rightarrow \beta'_1$ and $\beta_1 \rightarrow \gamma'_1$ known in *Cu-Al-Zn*-SMA's. The transformation $\beta_1 \rightarrow \gamma'_1$ takes place only under mechanical stress and can enter in this case as one of the

accommodation mechanisms – the minimization of the mechanical internal stresses developed during of the nucleation and the growing of β'_1-martensite crystals.

The pure lattice deformation (Bain's dilatation) exhibits different signs for one of the cubic axes ([100] is the longitudinal axis of our single crystal sample) during of these two transformations: the shortening in the case of $\beta_1 \rightarrow \beta'_1$-transformation and the elongation in the case of $\beta_1 \rightarrow \gamma'_1$-one. The latent transformation heat for these two transformations is nearly the same, so that they are not to be differentiated by calorimetry, as it also shows Fig. 5.1 c.

Another of the possible explanations of such jumps of the coefficient of the thermal expansion could consist in the fact that only the one $\beta_1 \rightarrow \beta'_1$-transformation causes that kind of dilatation by the entering accommodation mechanisms during the developing of the mechanical internal stresses called by the lattice deformation and accompanying every martensitic transformation and/or set only after the reaching a certain level of these stresses. The 1st (primary) mechanism is the secondary shifts of atomic plans – so-called deformation with the invariant crystal lattice – leading to the twins building, and the 2nd (secondary) mechanism is the growing together of martensite crystals, which leads to the building of complex groups of martensite crystals.

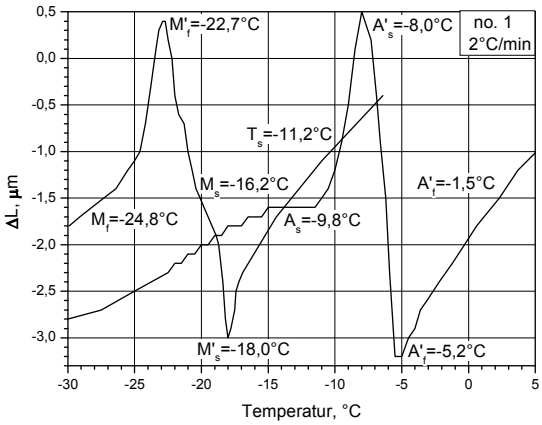

Fig. 5.1 a: Dependence of the length change of sample 1 (*Cu-Al-Zn*) on the temperature during direct and reverse transformations

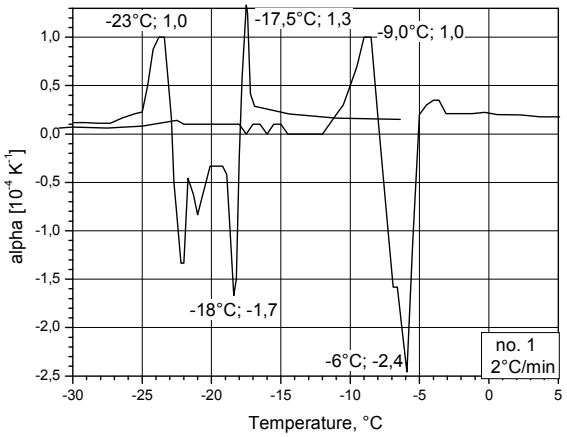

Fig. 5.1 b: Coefficient of thermal expansion (*Cu-Al-Zn*, sample 1) vs. temperature in the transition temperature range

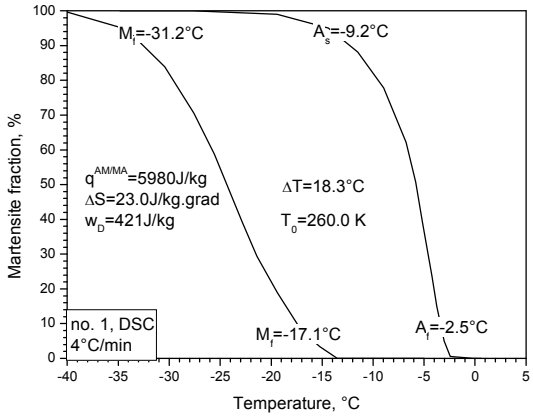

Fig. 5.1 c: Transformation hysteresis loop designed by calorimetry (sample 1)

However, it is speaking against such generally well-known accommodation mechanisms in this case both the dilatometric observing alternating effect of the lattice deformation and the accommodation processes, which normally run simultaneously, as well as the ratio between the negative (dilatation by the lattice deformation) and positive (dilatation recovery by the accommodation) values of length changes, which really should be smaller or alike 1 ($k = \left| \frac{\Delta L^+}{\Delta L^-} \right| \leq 1$).

The minimum length change or the minimum spontaneous deformation of the *Cu-Al-Zn*-sample (Table 5.1) points anyhow to the

very effective accommodation (by whatever mechanism always) of the lattice deformation, which causes the macroscopic martensitic deformation up to 8% (for orientation <100> [27]) measured at the stress-induced transformation in single crystals of these alloys (sample 1).

Cu-Al-Mn single crystal with orientation [110] of the length axis (sample 2) shows the greatest length change (Fig. 5,2 a, Table 5.1). But even this great deformation lies under the elastic strain limit in this alloy (ca. 0.013). The maximal martensitic deformation measured for this orientation on these samples under the tension experimentally [27] amounts about 5,0%.

The relation between the dilatation ε_d and the maximum martensitic deformation $\varepsilon_{\max}^M$:

$$k_n = \frac{|\varepsilon_d|}{\varepsilon_{\max}^M} \tag{5.4}$$

shows that about 25% of the lattice deformation was not accommodated or the accommodation degree k_a:

$$k_a = (1 - k_n) \cdot 100\% \tag{5.5}$$

amounts only about 75%.

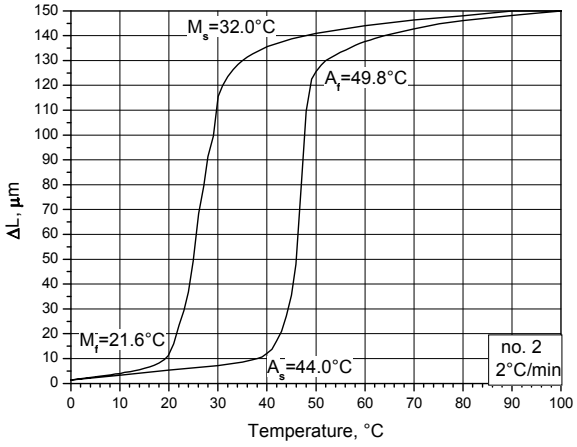

Fig. 5.2 a: Dependence of the length change (*Cu-Al-Mn*, sample 2) on the temperature during the direct and reverse transformations

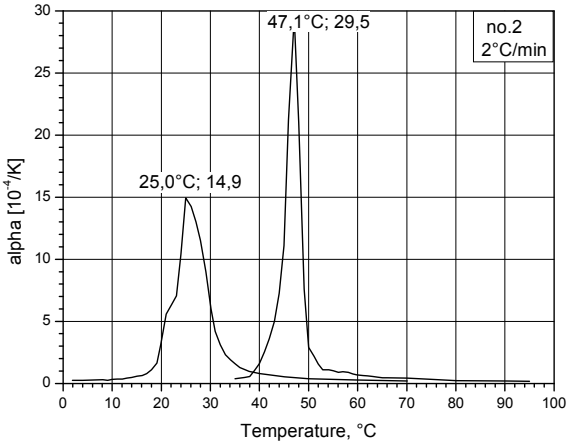

Fig. 5.2 b: Coefficient of the thermal expansion vs. temperature (*Cu-Al-Mn*, sample 2) in transition temperature range

The softening of the elastic shear modulus good well-known and before a long time experimental determined in this alloy, which minimized a critical shear stress in the systems {110} [110] in close proximity to the starting temperature of the martensitic transformation M_S is also promoting for a perfect accommodation of the lattice deformation. Shifts from atomic plans by the sliding of partial dislocations in these shear systems lead both to the primary lattice defor-

mation and thus to the martensitic transformation and to the secondary deformation with invariant lattice – to the twin building within a martensite variants as the 1st accommodation mechanism.

Since the twin building happens by shifts in the same shear system {110} [110], the non-accommodated lattice deformation within a martensite variant can be represented by different thickness of the opposite twin variants. If all twin pairs have the same thickness (a number of shear plans within a twin variant), the accommodation would be perfect ($k_a = 100\%$) and the resulting deformation equals zero.

The accommodation degree of 75% means that thickness ratio of positive (extension) and negative (shortening of the sample 2 toward <110>) twin variants amount to about 3/4. The same is valid for the 2nd accommodation mechanism: if all orientation variants of martensite crystals are equally presented in a single crystal sample with certain orientation of their longitudinal axis, the accommodation of the martensitic deformation would be perfect ($k_a = 100\%$)) and the dilatation along the longitudinal axis of the sample is zero.

This means that the whole lattice deformation has been accommodated perfectly by the 2nd accommodation mechanism. If the accommodation grade amounts about 75% as in the sample 2, this means that the number of martensite variants with negative contribution

to the sample dilatation on 25% would exceed the number of them with positive contribution. More to it will be further analysed in the discussion (chapter 6).

Such point of view of accommodation mechanisms and accommodation degrees puts the assumption nearly that the sign of the spontaneous deformation determined dilatometrically (shortening or extension of the sample during the direct transformation) may exhibit an arbitrary character, if none factors like e.g. internal stress affecting the further orientation of martensite variants are present in the sample.

The accommodation degree depends on the elastic characteristics like the value of the elastic modulus, determined also by its softening, and the value of the accommodated spontaneous deformation is limited by the yield, which may not be exceeded. Under this limit the non-accommodated spontaneous martensitic deformation can reach any value, affected probably by internal defect structure and internal stresses.

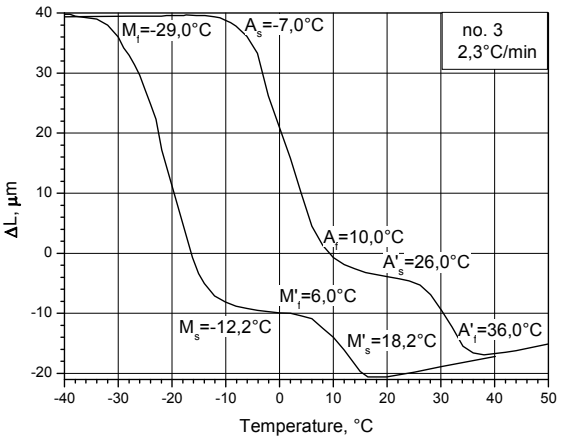

Fig. 5.3 a: Dependence of the length change (*Cu-Al-Ni*, sample 3) on the temperature during the direct and reverse transformations

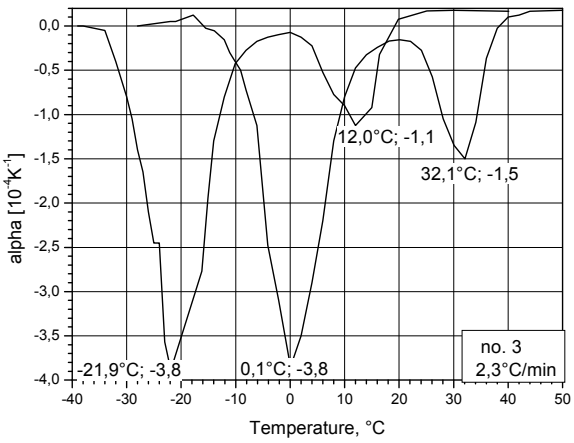

Fig. 5.3 b: Coefficient of the thermal expansion vs. temperature (*Cu-Al-Ni*, sample 3) in transition temperature range

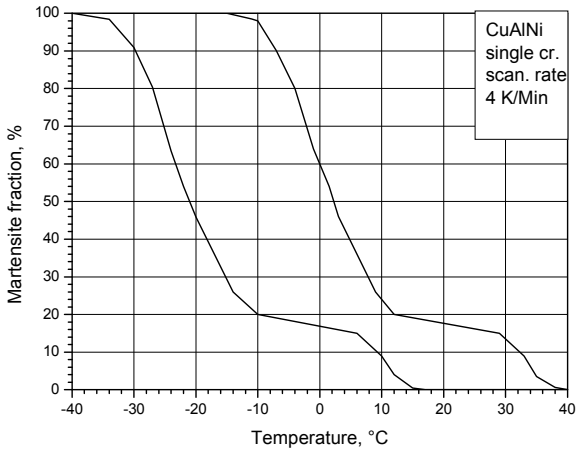

Fig. 5.3 c: Transformation hysteresis loop designed by calorimetry (sample 3)

This spontaneous dilatometric deformation of the single crystal sample 3 with the same orientation of its length axis, which however is caused by the martensitic transformation $\beta_1 \leftrightarrow \gamma'_1$, amounts only about half of that in the single crystal sample 2 (Table 5.1, Fig 5.3 a and b) but with the other sign ($\Delta L^{AM} > 0$, $\Delta L^{MA} < 0$ and $\alpha^{AM} < 0$, $\alpha^{MA} < 0$) like that in sample 4. The accommodation degree of the maximal martensitic deformation toward direction <110> (4% [25]) amounts to about 84% and, thus, substantially larger than that in sample 2.

The spontaneous dilatation ($\alpha^{AM} < 0$) of sample 4 – of the same alloy with the same orientation of the longitudinal axis only cut from a single crystal grown by another method – Is still smaller, only 0.15% (Fig. 5.4 a, 5.4 b and Table 5.1), and the accommodation degree of 96% is, thus, still larger. These differences by accommodation degrees are possibly be caused in these alloys just like softening of the elastic modulus in *Cu-Al-Zn*-SMA's.

The two-stage transformation, which was measured calorimetrically too (Fig. 5.3 c), is also indicated on the dilatometric hysteresis loop in sample 4 (Fig. 5.4 a), but only on the trajectory of the direct transformation. However, this has something to do rather with the single crystal quality (its homogeneity) and not with a sequence of different martensitic transformations or with anything accommodation specifics. It is also proved by the smaller hysteresis of the transformation in the single crystal sample 4, which obviously contains less defects than sample 3 and is more homogeneous.

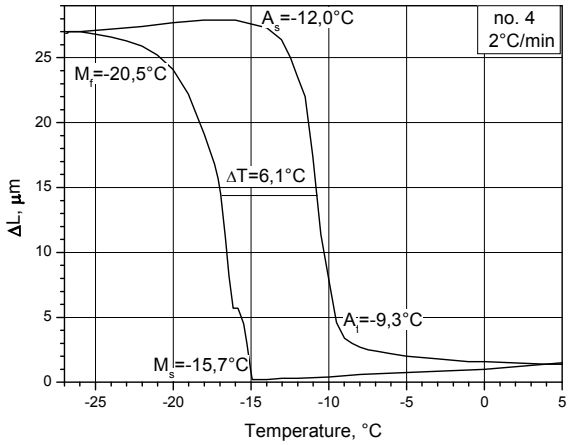

Fig. 5.4 a: Dependence of the length change (*Cu-Al-Ni*, sample 4) on the temperature during the direct and reverse transformations

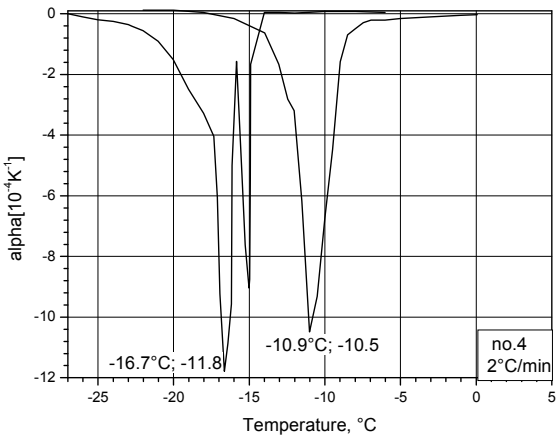

Fig. 5.4 b: Coefficient of the thermal expansion vs. temperature (*Cu-Al-Ni*, sample 4) in transition temperature range

5.1.2 Mn-Cu shape memory alloy with a magneto-structural transformation

As it already was mentioned above in 4.1, martensitic transformation of the face-centred cubic lattice of the paramagnetic matrix (austenite) into the face-centred tetragonal and antiferromagnetic ordered martensite ($fzc \rightarrow fct$) takes place in *Mn-Cu*-SMA, which is caused by the distorting effect (similar the magnetostriction in ferrous magnets) at the Neel's temperature

($T_N = T_t$) of the antiferromagnetically ordering atomic magnet moments and is coupled with this magnet transformation [25].

This means that the martensitic transformation takes place in the same temperature interval $M_S \le T_N = T_t \le A_f$ and both transformations exhibit the courses of transformations both 1st and the 2nd order: a very small hysteresis, a small jump the crystal lattice parameters at the transformation temperature and their monotonous change during the further cooling (Fig. 5.5 d).

The axis ratio in the tetragonal crystal lattice is $\frac{c}{a} < 1$, which causes a shortening of a single domain sample with orientation [001] of the length axis during the direct transformation. Exactly this is also observes with dilatation measurement under the temperature M_S (Fig. 5.5 a, Table 5.1).

It is something surprisingly for these "fine" transformation with relatively small lattice deformation $\varepsilon^M_{\max} = (1 - \frac{c}{a}) \approx 0{,}02$ comparable (with them of samples 2, 3, 4) large length change within the transition temperature range, although also this spontaneous deformation ($\varepsilon_d = 0{,}5\%$, Table 5.1) lies in the elastic strain range and appropriately agrees with the dilatation value of 0,5% [25] measured in the *Mn-Ni*-SMA with the same transformation mechanism. At the same as also in all other investigated alloys valid accommodation mechanisms (first of all the 1st mechanism) is the accommodation degree (5.5) $k_a = 75\%$ rather small like that in the sample 2. Thereby substantial softening of the elastic modulus in the pre-martensitic temperature interval of the paramagnetic matrix are experimental determined in this alloy in contrast to the alloy 2.

This large accommodated spontaneous deformation is obviously caused by the behaviour of the lattice deformation or the order parameters η specific for the transitions 2nd order, which can be introduced as ratio:

$$0 \le \eta = \frac{\varepsilon^M}{\varepsilon^M_{\max}} \le 1 \qquad (5.6)$$

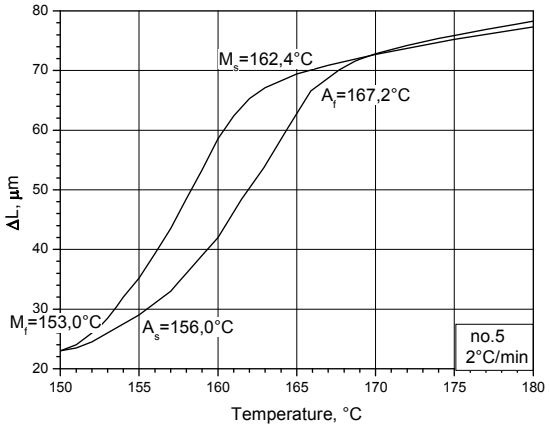

Fig. 5.5 a: Dependence of the length change (*Mn-Cu*, sample 5) on the temperature during the direct and reverse transformations

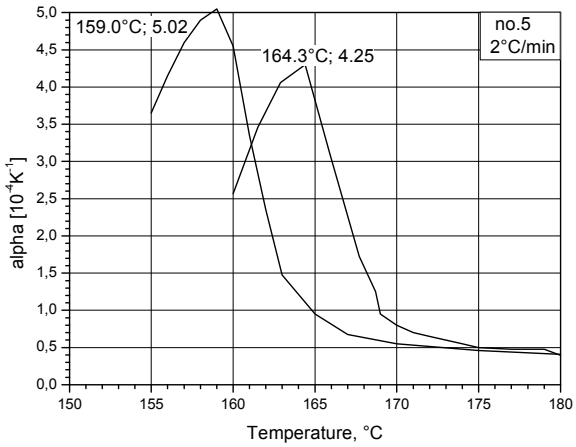

Fig. 5.5 b: Coefficient of the thermal expansion vs. temperature (*Mn-Cu*, sample 5) in transition temperature range

At the transition temperature $T_t \approx M_S$ only minimal jump of lattice deformation takes place, which lies in the elasticity range and should not be minimized at all by twin accommodation or should be only minimal accommodated, particularly already therefore that the transformation of whole volumes at the temperature T_t takes place and the two-phase state is hardly present.

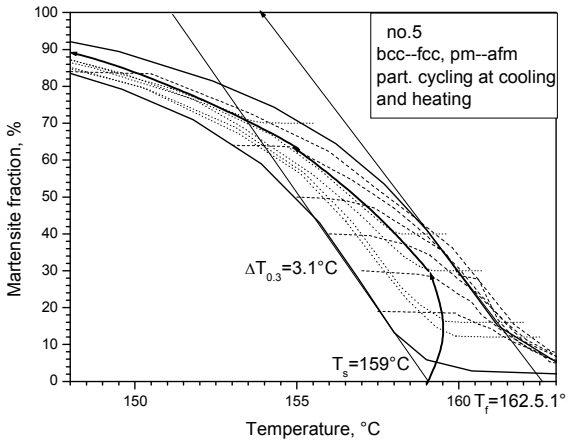

Fig. 5.5 c: Full hysteresis loop (sample 5) and the equilibrium line calorimetrically determined by the starting transformation temperatures in partial cycles

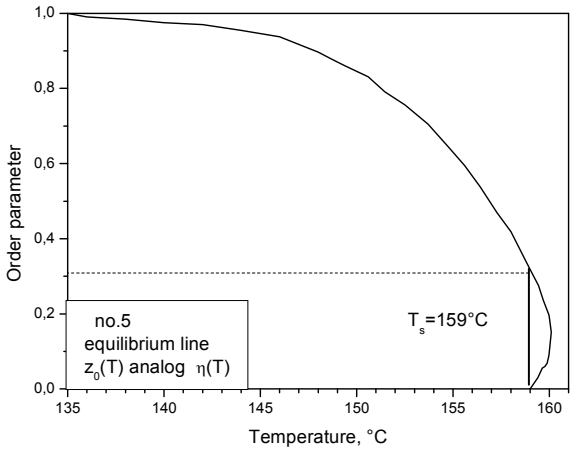

Fig. 5.5 d: Dependence of the order parameter on the temperature (sample 5)

During further temperature decreasing the order parameter increases to its maximal value. However, also this lattice deformation is accompanied by the heat spending, even if small, as it is usual for transitions of the 1st order.

The hysteresis loops determined calorimetrically by the measurements of the latent heat in full and partial transformation cycles are represented on the Fig. 5.5 c. The phase equilibrium line, which runs through the starting temperatures of direct and revers transformations in partial transformation cycles, corresponds qualitatively and quantitatively to the temperature dependence of the order parameter (eq. (5.6), Fig. 5.5 d).

In this way the deformation jump at the starting temperature the martensitic transformation can be calculated from Fig. 5.5 d at $z \approx 0.3$:

$$\Delta\varepsilon^{M}(T_t) = 0.02 \cdot 0.3 \approx 0.006 \qquad (5.7)$$

It can be seen from (5.7) that this value lies far away from the elastic limit. At the temperature about 140°C approaches the order parameter its maximal value. These calorimetric determined data agree with those from the dilatometry (Fig. 5.5 a) in the kind of the length change vs. temperature curves within the temperature interval of the transformation.

Such development of the transformation determines also real asymmetry ($A_H = \frac{\alpha^{AM}}{\alpha^{MA}} = 1.2$) of the hysteresis loop (Fig. 5.5 a and b, Table 5.1) with somewhat more expanded reverse transformation, because transformation trajectories runs at $\eta \to 1$ together and at $\eta = 0.3$ ($T = T_t$) they are separated by a relatively narrow temperature hysteresis. Otherwise, the coefficients of the linear thermal expansion of the austenite and the martensite are substantially larger than these in other samples.

5.1.3 TiNi shape memory alloys

TiNi SMA's with the *B2*-ordered austenite show different sequences or overlaps of martensitic transformations depending on their composition in the stoichiometric range. The main transformation $B2 \to B19'$ (*B2*-Austenit into the *B19* ordered martensite with monoclinic distorted orthorhombic crystal lattices) provides for large reversible deformation.

The best memory properties of these alloys compared with those of other SMA's are ensured however by interaction of $B2 \to B19'$ transformation with $B2 \to R$ transformation, whereby R designates a rombohedric structure, which is realized by atomic shifts {111} [112]

in *B2* structure. The $B2 \rightarrow R$ -transformation is considered as a transition like to those of the 2nd order due to a small (about 3°C) hysteresis. It leads likewise to reversible deformation of approximately 2%, while that by $B2 \rightarrow B19'$ -transformation amounts about 5%.

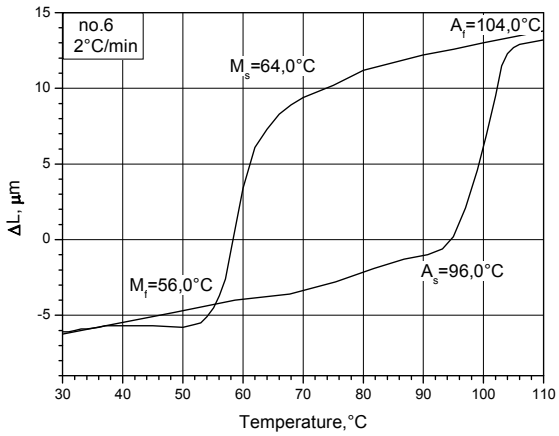

Fig. 5.6 a: Dependence of the length change on the temperature during the direct and reverse $B2 \leftrightarrow B19'$ transformations (*TiNi*, sample 6)

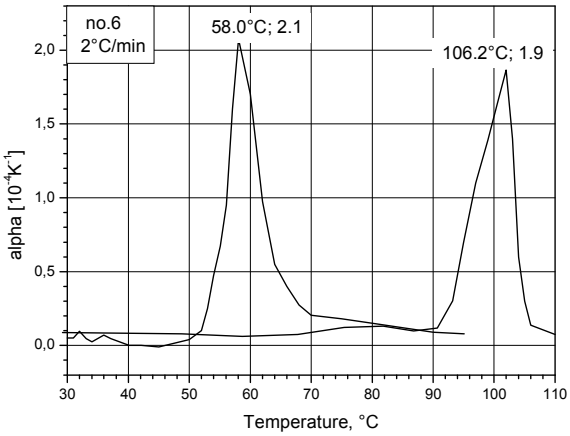

Fig. 5.6 b: Coefficient of the thermal expansion vs. temperature in transition temperature range (*TiNi*, sample 6)

In the equiatomic alloy $Ti_{50}Ni_{50}$ (sample 6) only the transformation $B2 \rightarrow B19'$ is observed, while the transformation $B2 \rightarrow R$ runs parallel in the background and can be only in partial cycles separated from $B2 \rightarrow B19'$ [23]. Dilatometric curves for direct and revers transformations form a typical for $B2 \leftrightarrow B19'$-transformations nearly symmetrical ($A_H = 1{,}1$) and wide (37°C) hysteresis loop (Fig. 5.6 a and b, Table 5.1).

The dilatation ($\alpha^{AM} > 0$) of polycrystalline, but by rolling textured [28] and cut crosswise to the rolling axis sample is relatively small ($\varepsilon_d = 0.0016$). The accommodation degree k_a amounts thus of more than 97%. The nearly complete accommodation of the lattice deformation during the martensitic transformation in *TiNi* SMA's is well-known, whereby the 2nd accommodation mechanism - formation of complex groups from the grown together martensite variants is here particularly effective. This accommodation ability together with substantial softening of the elastic modulus contributes for their part to perfect memory properties of these alloys.

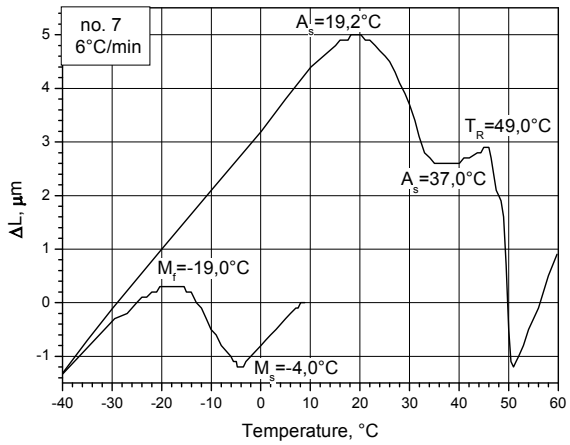

Fig. 5.7 a: Dependence of the length change on the temperature during $B2 \rightarrow R \rightarrow B19'$ direct and $B19' \rightarrow R \rightarrow B2'$ reverse transformations (*TiNi*, sample 7)

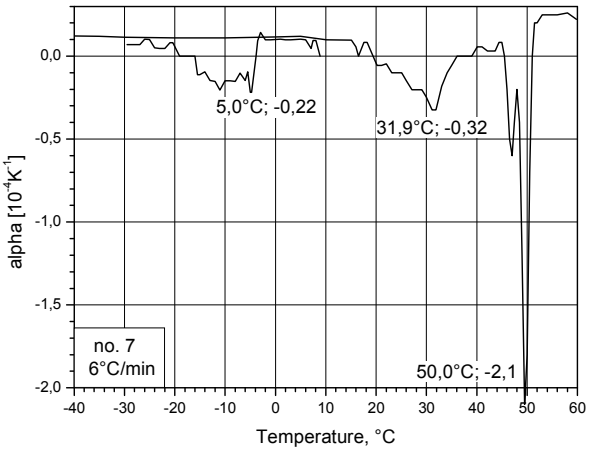

Fig. 5.7 b: Coefficient of the thermal expansion vs. temperature in transition temperature range (*TiNi*, sample 7)

At the cooling of the martensitic phase just under the temperature M_f the coefficient of the linear thermal expansion equals zero in a temperature range about 10°C ($40 \div 50°C$). Thus, the martensitic phase in this SMA points, as the martensitic phase sample 3 too, but in much broader temperature range the so-called invare behaviour. The coefficients of the linear thermal expansion of the austenite and the martensite are each other alike, have however a value like one of the sample 1, which is substantially smaller than these of all other investigated hear SMA's.

In *TiNi* SMA with higher *Ni*-content, like that in sample 7, temperatures of $B2 \rightarrow B19'$-transformation drastically sinks, while those of $B2 \rightarrow R$-transformation are hardly affected. Thus, the temperature ranges of the two transformations separate in such a way that the transformation sequence $B2 \rightarrow R \rightarrow B19'$ is realized (Fig. 5.7 a und b).

At this transformation sequence the sample elongates during both $R \rightarrow B19'$-transformation ($\alpha^{R \leftrightarrow B19'} < 0$), and $B2 \rightarrow R$-one ($\alpha^{B2 \leftrightarrow R} < 0$). The resulting spontaneous deformation of the sample is still smaller than those in sample 6, whereby this deformation caused by $B2 \leftrightarrow B19'$-transformation is even smaller than the dilatation caused by $B2 \leftrightarrow R$-one ($\varepsilon_d^{B2 \leftrightarrow B19'} = 0.0002$, Table 5.1).

The accommodation degree of the lattice deformation at these transformations approaches 100% ($k_a^{B2\leftrightarrow B19'} \approx 99.7\%$, $k_a^{B2\leftrightarrow R} \approx 99.0\%$), and is, thus, a perfect accommodation. It can be caused by very small values of the elastic modulus, what accordingly causes small critical shear stresses in the shear system and a small energy of staking faults and relieves the twin building needed for the 1st accommodation mechanism

5.2 Scanning rate

As it has been determined at calorimetric investigations [15], the scanning rate (velocity of the temperature change) affects the transformation temperatures very strongly, so that both the width of internal, latent hysteresis ($A_S - M_S$) and the two-phase temperature ranges ($M_S - M_f$ and $A_f - A_S$) increase continually with increasing of the scanning rate. This problem has fundamental meaning for the shape memory actuators, because their response time becomes ever longer. Substantial aiming are everywhere undertaken to reduce drastically this response time by the miniaturization of SMA actuators [29] and by more effective cooling methods [30].

In our work is looked for the answer to the question: whether the velocity of the martensitic transformation in SMA's is physically limited, speak whether these transformations lets principally boundless accelerate by miniaturization, more effective cooling and others cheats? There are also enough of publishes experimental data, which agree with our calorimetric results and prove this velocity limit by the expansion of the critical range both of thermal and stress induced transformation with the increasing of the scanning rate.

It was one aim of this work to examine the calorimetric result [15] by the using of another measuring method, which lets directly measure mechanical reaction of a SMA sample on its temperature change. In a calorimeter the velocity of the transformation is not measured directly, but the latent transformation heat and its flow, which time-delayed could be measured even then in the sample, if the transformation already is to end [20].

This contradicts the thermo-elasticity model of the martensitic transformation in SMA's, after which the thermo-elastic martensitic transformation continues only with temperature changes and rests at each temperature stop. It was however proved experimentally [20] that the reverse transformation already was to end while calorimetric measured endothermic heat flow corresponded still to the remainder martensite quantity up to 30%. It is particularly actually for transformations with a small hysteresis ($B2 \leftrightarrow R$, $B2 \leftrightarrow B19$ transformations in *TiNi* basis polycrystals as well as in *TiNi* and *Cu-Al-Zn* single crystals.

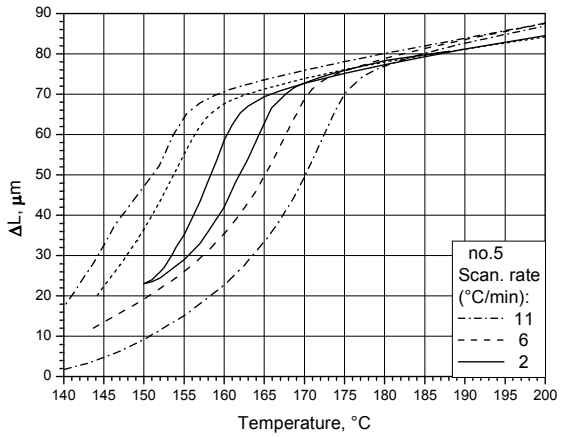

Fig. 5.8 a: Dependences of the length change *(Mn-Cu*, sample 5) on the temperature at different scanning rates

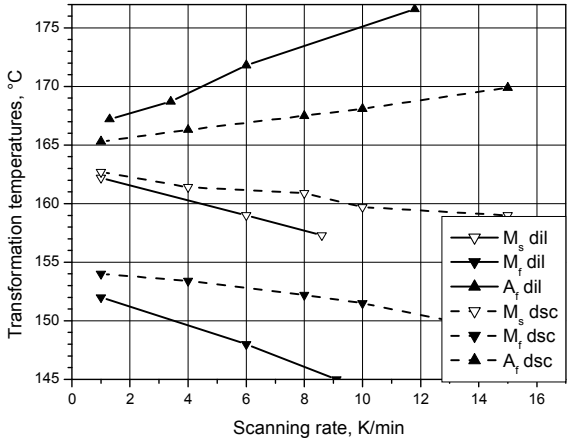

Fig. 5.8 b: Transformation temperatures determined dilatometrically (dil) und calorimetrically (dsc) vs. scanning rate (sample 5)

At the dilatation measurements the reaction (length change) vs. the temperature change is recorded, which is connected directly - without time delaying - with the transformation. Like the dilatometric curves represented in Fig. 5.8 a for sample 5 showed as example, the expanding of the transformation temperature range is in all investigated alloys still larger than that measured calorimetric (Fig. 5.8 b).

Finish temperatures of the direct and the reverse transformations determined from measured curves similar those in Fig. 5.8 a are represented on Fig. 5.9 a and b. The finish temperatures are important because they limiting the whole critical range, in which a full transformation cycle at the cooling up to M_f-temperature (there) and at heating up to A_f-temperature (back) takes place. The time t needed for it will be calculated through this temperature range $(A_f - M_f)$ and the scanning rate $\dot{T}$:

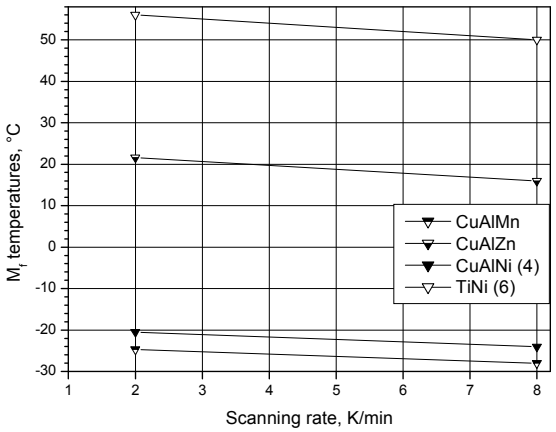

Fig. 5.9 a: Finish temperatures of the direct transformations vs. scanning rate (samples 1, 2, 4 and 6)

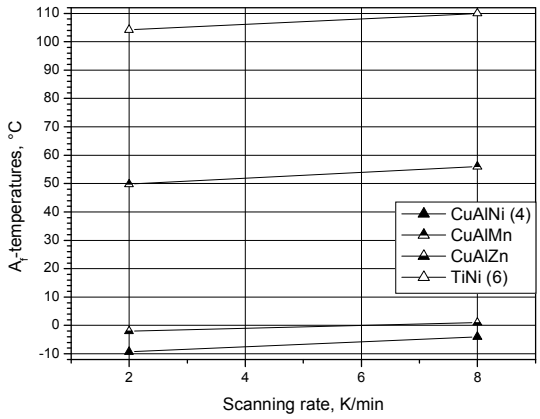

Fig. 5.9 b: Finish temperatures of the direct transformations vs. scanning rate (samples 1, 2, 4 and 6)

$$t = \frac{2(A_f - M_f)}{\dot{T}}, \tag{5.8}$$

and the working frequency f of a SMA-actuator is accordingly defined as follows:

$$f(Hz) = t^{-1} \tag{5.9}$$

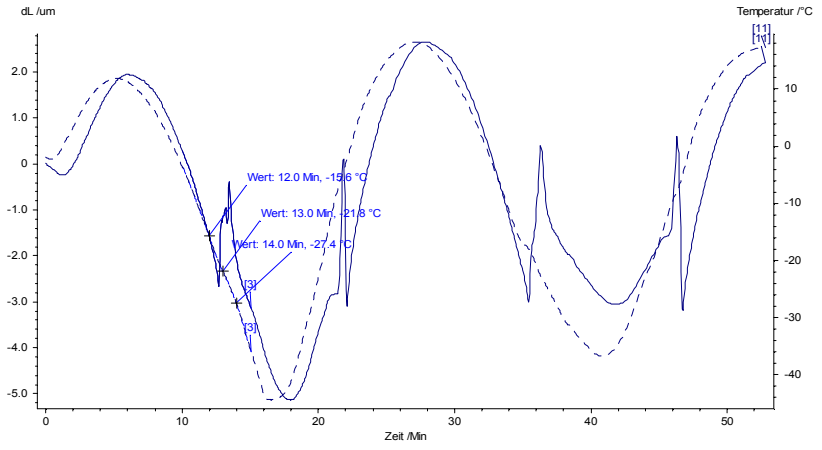

Fig. 5.10: Dilatometric curves $\Delta L(t)$ and $T(t)$ measured at different scanning rate on the sample 1

Thus, the physical limiting of the working frequency of SMA-actuators is also determined dilatometrically. It is connected – as already assumed in [15] – with brakes of phase boundaries by the own latent transformation heat and its removal. The closer the transformation conditions to adiabatic are, (infinitely large scanning rate), the more incompletely is the martensitic transformation, until this

is then blocked completely and at all does

not take place any longer.

However, it again remain doubts due to possible methodical artefacts. It can be seen on the dilatation measuring curves (Fig. 5.10) that the length change (the reaction) takes place always time-delayed relative the signs change of the scanning rate (from cooling to heating), whereby the time delay lies in the minute range.

In the $T(t)$-function T is the temperature measured on the surface of the dilatometric sample, which is much more massive compared with calorimetric one, whereas $\Delta L(t)$ represents the volume reaction of the whole massive sample on the temperature change within this volume.

This time delaying is caused by the time needed to reaching of the temperature equilibrium between the sample surface and the centre of the massive ($2{,}0x2{,}5x10{,}0\,mm^3$) sample by means of the thermal conduction.

Such time delaying cannot unfortunately be measured methodically in the calorimeter for much more smaller samples (disks Ø4,0 *mm* and thickness of 1,0 *mm*) with direct contact to the heat transferring ground of the measuring chamber.

Anyway the same problem exists also for SMA-actuators under real work conditions, which one tries to solve by actuator miniaturization.

6 Discussion

6.1 Dilatometry of shape memory alloys

6.1.1 Thermal expansion of the austenite and the martensite

The dilatation behaviour of the austenite and the martensite in SMA in temperature ranges $T > A_f$ and $T < M_f$ correspondently, thus outside of the two-phase range, is determinated by the temperature behaviour of the elastic modulus $\alpha = -\frac{k_1^{-1}}{G_0} \cdot \frac{dG}{dT}$, like it has been described in chapter 3 (eq. 3.24), and does not differ under normal conditions ($\frac{dG}{dT} = const < 0$) from that of the other metal alloys.

Since the elastic modulus of the austenite and the martensite are each other alike ($G_0^A = G_0^M$), the coefficients of the thermal expansion of the two phases likewise are each other equivalent ($\alpha^A = \alpha^M$), so long $\frac{dG^A}{dT} = \frac{dG^M}{dT}$.

This applies, as it show the dilatometric results (Tab. 5.1) only in samples 2 and 6. For sample 4 it is valid $\alpha^A < \alpha^M$ and for samples 1, 3, 5 and 7 – vice versa $\alpha^A > \alpha^M$. The martensite in sample 3 is in a broad temperature interval $T < M_f$ invar ($\alpha^M = 0$), while the coefficient of the linear thermal expansion of the austenite has a normal value for this SMA.

An anomaly behaviour (softening) of the elastic modulus of the austenite is determined in a pre-martensitic temperature range $\Delta T = T_S - M_S$ in the most SMA's, like *Cu-Zn-Al* and *TiNi* e.g. The temperature dependence of the module reaches its maximum at a temperature T_S and gets a positive temperature coefficient $\frac{dG^A}{dT} > 0$, so that the elastic modulus decreases during the temperature decreasing up to the start temperature M_S of the direct martensitic transformation.

After that the elastic modulus of the martensite increases rapidly to its normal values at these lower temperatures with again normal negative temperature coefficients.

It follows from the equation (3.24) that the coefficient of the thermal expansion with so an anomaly behaviour of the elastic modulus should change its sign at the temperature $T_S > M_S$, so that at $T > T_S$: $\alpha^A > 0$, at $T = T_S$: $\alpha^A = 0$ and at $T_S > T > M_S$: $\alpha^A < 0$. As the results of the Table 5.1 show, a negative coefficient of the thermal expansion of the austenite is observed in none of the investigated SMA's.

As far as the relationship between α^A and α^M goes, it seems to agree with the softening concept only in sample 4 due to the rapid increasing of the elastic modulus within the range $T < M_f$. The case $\alpha^A > \alpha^M$ is rather unusual for this concept.

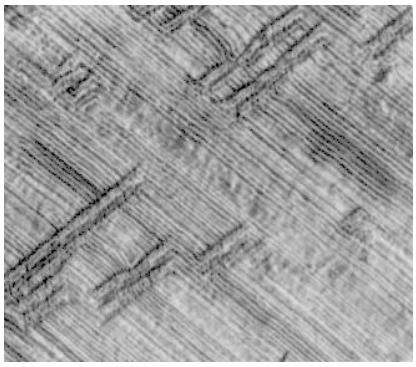

Fig. 6.1 a: Dynamic schear structures in *B2*-austenite within pre-martensitic temperatur range (sample 1, x200.000)

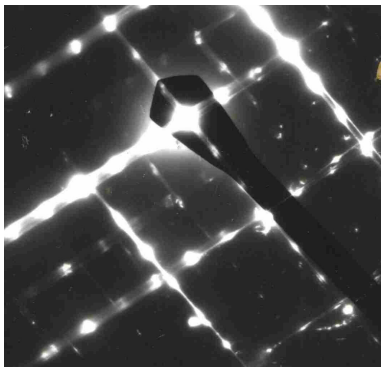

Fig. 6.1 b: Electron diffraction with diffuse 1/3<110> extra-reflexes from the same region in *B2*-austenite, foil surface $(110)_{B2}$

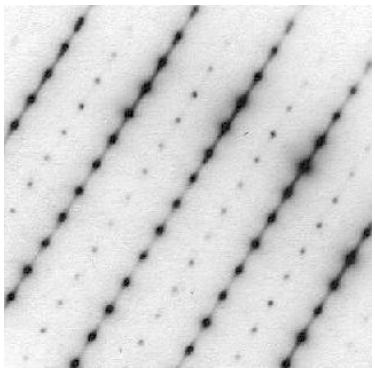

Fig 6. 1 c: Electron diffraction from *9R*-martensite of sample 1 (Fig. 6.3 a), foil surface $(110)_{9R}$

The determined inequality of the expansion coefficients of the martensite and the austenite $\alpha^A \neq \alpha^M$ permits to draw a fundamental conclusion about different dependence of the entropy of the two phases on external stress. It follows from equation (3.15):

$$\alpha^A - \alpha^M = \frac{1}{\varepsilon} \cdot \frac{d(S^A - S^M)}{d\sigma} = \frac{1}{\varepsilon} \cdot \frac{dS^{AM}}{d\sigma} \tag{6.1}$$

This means that the Claypeyron-Clausius' equation (3.4) in their this form is not correct for SMA's in the case of $\alpha^A \neq \alpha^M$, thus $S^{AM} = f(\sigma)$.

The result that the coefficient of thermal expansion of the austenite does not exhibit negative values in the temperature interval $T_S > T > M_S$ – If such exists at all – can be explained only by the fact that dynamic-periodic shear structures have already formed within the same interval as harbingers of the coming shear transformation, which is giving a larger positive contribution to the coefficients of the thermal expansion than those from the elastic modulus, how it is also the case in two-phase temperature range. Such dynamic shear structures had been also observed in *Cu* basis SMA's on electron-micrograms and difractograms (Fig. 6.1 a, b and c)

6.1.2 Thermal expansion in two-phase temperature region

Since the entropy of the martensite is smaller than the one of the austenite, the change of entropy is negative in the two-phase temperature range $\Delta S^{AM} = S^A - S^M < 0$. If the martensitic transformation is caused by external stress (stress-induced transformation), this means thus followed to equation (3.15):

$$\frac{dS^{AM}}{d\sigma} < 0 \text{ und } \alpha^{AM} < 0. \tag{6.2}$$

The negative values of the coefficient of the thermal expansion are valid also in the two-phase range of the thermo-induced martensitic transformation, because this coefficient characterizes the material state and not the way, in which the material accepts this state. This means that the length of the sample from a shape memory alloy increases during the direct martenitic transformation and decreases during the reverse transformation, even if no transformation-specific changes of volume and/or of length are present.

Since the elastic modulus G^{AM} of the two-phase state (2.1) behaves at the condition $G^A = G^M$ like the one of the pure phases, it is to expect a positive contribution from the connection (3.24) to the coefficient of the linear thermal expansion in the two-phase temperature range, because the thermal coefficient both of the austenite $\frac{dG^A}{dT}$ and of the martensite $\frac{dG^M}{dT}$ became negative after the reaching of the starting temperature M_S at the cooling. The increasing of the elastic modulus at the temperature decreasing after M_S is larger than normal, if the softening of the elastic modulus $\frac{dG^A}{dT} > 0$ took place before M_S-temperature. Thus, softening of the elastic modulus in the pre-martensitic temperature range is to entail a positive change of the sample length at the cooling in the two-phase temperature range.

Since the experimental results in this work show both from these cases - also in samples with martensitic transformations of the same kind, with the equal transformation entropy and with the same behaviour of the elastic modulus, the value and the sign of the coefficient of the thermal expansion in the two-phase temperature range should be determine by other factors.

6.1.3 Contributions of the lattice deformation after its accommodation

The behaviour of the coefficients of the thermal expansion in two-phase temperature ranges $M_S > T > M_f$ and $A_S > T > A_f$ can be changed drastically by the length change of the sample in certain directions due to the lattice deformation of the martensite. The resulting spontaneous deformation ε_M not compensated by the building of internal twins inside of one martensite variant (Fig. 6.2 and 6.3 a) can be determined as follows:

$$\varepsilon_M = tg\vartheta = \gamma(1 - \nu_{tw}) \tag{6.3}$$

whereby $\gamma = tg\beta$ is the primary martensitic shear deformation or lattice deformation and

$$\nu_{tw} := \frac{n^-}{n^+} \tag{6.4}$$

is the twinning degree of a martensite variant or the accommodation degree reached by the 1st accommodation mechanism.

The number of secondary (invariant) shifts of atomic plains in the martensite variant $n^- = N - n^+$, which lead to the building of internal twins in the martensite variant consisting of *N* shear atomic plains, depends a priori on the mechanical shear stress τ affecting this twin polydomain in the shear plain:

$$\tau = \sigma \cdot \cos\phi \cdot \cos\varphi = \sigma \cdot \mu\,, \tag{6.5}$$

whereby σ is external stress affecting along the sample axis or also internal stress effecting on a martensite variant from its environment, ϕ and φ are the angles between the length axis of the single-crystal sample and the normal to the shear surface and between the length axis and the shear direction, μ is so-called orientation factor (at $\phi = \varphi = \frac{\pi}{4}$ and $\tau = \frac{1}{2}\sigma = \tau_{\max}$).

The resulting shear deformation ε_M (6.3) causes a relative measurable in a dilatometer length change of a sample $\frac{\Delta L}{L_0} \equiv \varepsilon_d$ consisting only from this individual martensite variant, which is likewise determined by the orientation factor μ:

$$\varepsilon_d = \mu \cdot \varepsilon_M \tag{6.6}$$

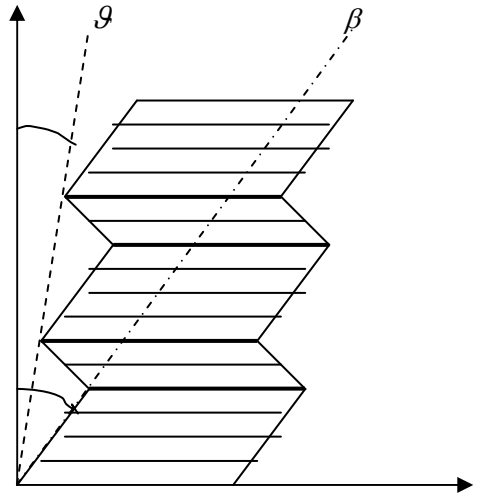

Fig. 6.2: Twins building in a single martensite variant consisting of *N* atomic plains (bold lines are internal twin boundaries)

In the two-phase range with a mass fraction (phase fraction) of the martensite:

$$z = \frac{m_M}{m_A + m_M} = \frac{m_M}{m}, \qquad (6.7)$$

(m_M, m_A, m are appropriate masses of the martensite, of the austenite and of the whole sample) the length change of the sample $\pm\Delta L$ (sign $\pm$ means elongation or shortening of the sample depending on the direction of the entire not compensated lattice shear deformation in the martensite) completely measured in the dilatometer and directly caused by the martensitic transformation depends on the phase fraction of the martensite as the deformation causer:

$$\frac{\Delta L}{L_0} = \mu \cdot \gamma (1 - \nu_{tw}) \cdot z \qquad (6.8)$$

The contribution $\alpha_\varepsilon^{AM/MA}$ of the martensitic deformation to the coefficients of the thermal expansion along the sample length axis in the temperature interval of the martensitic transformation (two-phase temperature range – upper index *AM* and *MA*) is then:

$$\alpha_\varepsilon^{AM/MA} = \frac{1}{L_0} \cdot \frac{d(\Delta L)}{dT} = \mu \cdot \gamma (1 - \nu_{tw}) \cdot \frac{dz}{dT} - \mu \cdot \gamma \cdot z \cdot \frac{d\nu_{tw}}{dT}, \qquad (6.9)$$

whereby $\frac{dz}{dT} < 0$ is the slope of the hysteresis loop $z(T)$ determined calorimetrically, which is always negative, whereas the orientation factor μ can be both negative and positive. It is to presume that the twinning degree in individual martensite variants can only decrees by their elastic interaction during the increasing of the phase fraction of the martensite *z* (2nd accommodation mechanism) with the temperature decreasing ($\frac{d\nu_{tw}}{dT} < 0$, otherwise the 2nd term in (6.9) is zero).

If $\frac{d\nu_{tw}}{dT} = 0$, the sign before the coefficients of the linear thermal expansion (negative or positive) would be determined by the first term in (6.9). Here $\frac{dz}{dT} < 0$, $(1 - \nu_{tw}) > 0$ always and:

1. $\alpha_\varepsilon^{AM/MA} > 0$ (samples 1, 2, 5. 6), if $\mu < 0$, thus only then if $270° > \phi > 90°$ and $90° > \varphi > 0°;\ 0° > \varphi > 270°$ ($\cos\phi < 0$ and $\cos\varphi > 0$) and thus $\mu < 0$.

2. $\alpha_\varepsilon^{AM/MA} < 0$ (samples 1, 3, 4, 7), if $\cos\phi > 0$ and $\cos\varphi > 0$ or $\cos\phi < 0$ and $\cos\varphi < 0$ and thus $\mu > 0$.

These two cases arise with the same probability, if no oriented affecting internal or external stresses present in the sample.

It is thereby obviously that the purely physical entropy and elasticity effects, discussed above, remain in the background of the transformation and only accommodation causes the changes of the coefficients of the thermal expansion in two-phase temperature ranges and go into action only if the accommodation is nearly perfect.

It follows from the equation (6.9) that $\alpha_\varepsilon^{AM/MA} = 0$, if $\nu_{tw} = 1$ or $\mu = 0$ ($\varphi = \frac{\pi}{2}$ – all martensite variants are oriented perpendicular to the sample length axis) and $\frac{d\nu_{tw}}{dT} = 0$. The latter means the fact that the number of positive and negative twin variants as well as their thickness are each other equal, the martensitic lattice deformation is thereby perfectly accommodated

within single martensite variants and this condition does not change by the elastic interaction of different martensite variants.

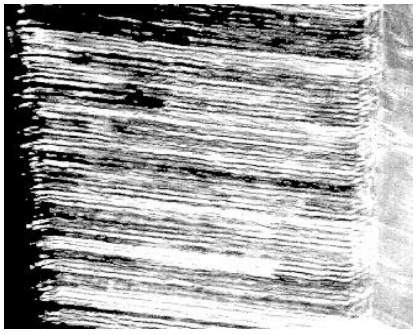

Fig. 6.3 a: A single martensite variant with internal twins (x50.000)

Fig. 6.3 b: A wedge-shaped martensite plate grown together from two martensite variants (x50.000)

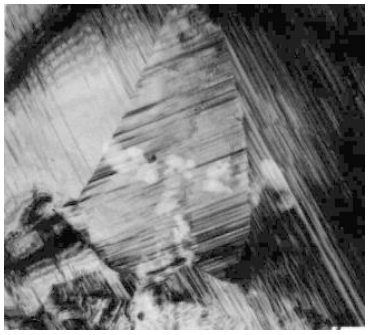

Fig. 6.3 c: A martensite complex grown together from several variants (x50.000)

The twin building within a single martensite variant is the primary accommodation mechanism during martensitic transformations, that serves the reduction of elastic stresses τ on the phase boundaries, if they reach the critical stress τ_{tw} needed for the twin building, which lies under the yield τ_y:

$$\tau = \tau_{tw} < \tau_y \,. \tag{6.10}$$

This accommodation mechanism ensures the coherence of phase boundaries in SMA's and thus their mobility – one of the most important characteristics, which is the basis for the shape memory effect in all its features.

Thus, the contribution (6.9) is not to be neglected at dilatation measurements, even if it lies in the elastic deformation range ($\varepsilon_y < 1{,}5\%$), because it results in even at $\varepsilon_M = 0{,}5\%$ or $\frac{\Delta L}{L} = 0{,}005$ in the two phase temperature interval of the martensitic transformation (approximately 10°C) an expansion coefficient of 500x10^{-6} K^{-1}, while the normal coefficient of thermal expansion for metals in their single phase state amounts about only 17x10^{-6} K^{-1} (for *Cu*).

The 2nd accommodation mechanism is realized by the interaction and growing together of differently oriented martensite variants (Fig. 6.3 b and c), relieves each single martensite variant from internal stresses developing on the austenite-martensite phase boundaries through their transforming into the internal martensite-martensite boundaries, and can lead thus to the reduction of the twin density ν_{tw} within single martensite variants.

In the Table 6.1 are listed all deformation contributions from shifts in all possible shear systems toward <110>-axis (projections on this axis), which form 12 differently oriented martensite variants. It is comprehensible from the Table 6.1, how negative or positive deformation of the sample toward <110>-axis are realized and how a full or partial accommodation of the martensitic deformation ε_M within the whole sample volume takes place by interaction and growing together of differently oriented martensite variants. Fig. 6.3 b shows for example one martensitic plate consisted from two grown together martensite variants with shear system oriented perpendicularly to each other: $(101) < 101 >$ and $(\bar{1}01) < \bar{1}01 >$. Their shear deformations $+0.5\varepsilon_M$ and $-0.5\varepsilon_M$ compensate each other on the common martensite-martensite boundary (001) – so-called habitus plain of the resulting martensite plate.

Table 6.1 Deformation contributions from shifts in all possible shear systems toward <110>-axis

Shear plain	(110)	$(\bar{1}10)$	$(1\bar{1}0)$	$(11\bar{0})$	(101)	$(10\bar{1})$
Shear direction	$<110>$	$<\bar{1}\bar{1}0>$	$<\bar{1}10>$	$<1\bar{1}0>$	$<101>$	$<\bar{1}0\bar{1}>$

Deformation toward <110>	$+\varepsilon_M$	$-\varepsilon_M$	0	0	$+0.5\varepsilon_M$	$-0.5\varepsilon_M$

Table 6.1 Continuation

Shear plain	$(\bar{1}01)$	$(\bar{1}01)$	(011)	(011)	$(0\bar{1}1)$	$(0\bar{1}1)$
Shear direction	$<\bar{1}01>$	$<10\bar{1}>$	$<011>$	$<0\bar{1}\bar{1}>$	$<0\bar{1}1>$	$<01\bar{1}>$
Deformation toward <110>	$+0.5\varepsilon_M$	$-0.5\varepsilon_M$	$+0.5\varepsilon_M$	$-0.5\varepsilon_M$	$+0.5\varepsilon_M$	$-0.5\varepsilon_M$

All transformation specialities discussed above including heat effects and accommodation processes determine transformation kinetics, which does not necessarily have to be athermal and in this sense thermo-elastic, and velocity of the martensitic transformations in SMA's, which is much smaller than the sound velocity of the classical martensitic $\gamma \rightarrow \alpha$ -transformation in steel at its quenching.

6.2 Physical limiting of the transformation velocity

6.2.1 Transformation frequency and stationary transformation

The transformation velocity and/or the transformation frequency (the number of complete transformation cycles per second in *Hz*) calculated from real, calorimetric measured transformation temperature interval $M_f \div A_f$ [15] depends logarithmically (Fig. 5.4 a) on the scanning rate and reaches anything as saturation within the range of approx. 0.06 *Hz* ($B2 \leftrightarrow B19'$) up to approx. 0.012 *Hz* ($B2 \leftrightarrow B19$), thus far away under the 1*Hz*-limit. In massiv dilatometry samples this frequency limiting is still stronger (Fig. 6.4 b).

A linear extrapolation of the transformation temperatures (Fig. 5.8 b) of sample 5 toward $\dot{T} = 0$ (stationary transformation condition) results (Table 6.2) in the real stationary width values

Table 6.2 Hysteresis loop characteristics of sample 5 extrapolated to zero scanning rate

$M_s^c(0)$	$M_s^d(0)$	$M_f^c(0)$	$M_f^d(0)$	$A_f^c(0)$	$A_f^d(0)$	ΔT_h^c	ΔT_h^d	ΔT_M^c	ΔT_M^d	ΔT_t^c	ΔT_t^d
163,0	163,0	154,0	153,0	165,0	165,5	2,5	3,0	9,0	10,0	22,0	25,0

of the hysteresis ($\Delta T_h^{c,d} = A_f^{c,d}(0) - M_s^{c,d}(0)$), of the two-phase temperature intervals ($\Delta T_M^{c,d} = M_s^{c,d}(0) - M_f^{c,d}(0)$) and of the temperature interval of a complete transformation cycle ($\Delta T_t^{c,d} = 2 \cdot [A_f^{c,d}(0) - M_f^{c,d}(0)]$) without the adiabatic contribution achieving with rising scanning rates (dynamic conditions). The extrapolated temperature values hardly differ in dilatometry (high index *d*) and calorimetry (high index *c*).

Stationary transformation conditions mean the absence of relaxation processes during the transformation including the temperature equalizing at the phase boundary as source of the latent transformation heat with the environment, or independence of all transformation parameters on the time (all time derivatives are zero), so that kinetics of the transformation is determined only by the own velocity of phase boundaries.

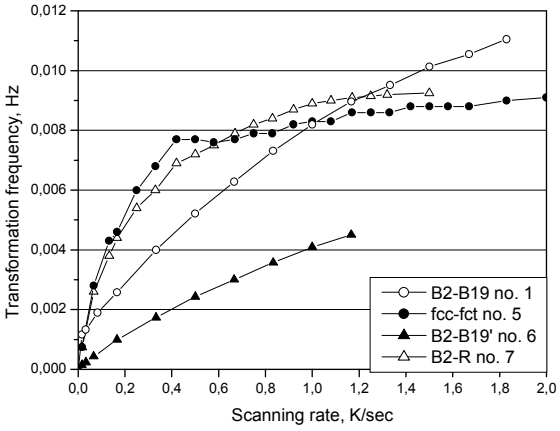

Fig. 6.4 a: Dependences of transformation frequencies on the. scanning rate (samplea 1, 5-7)

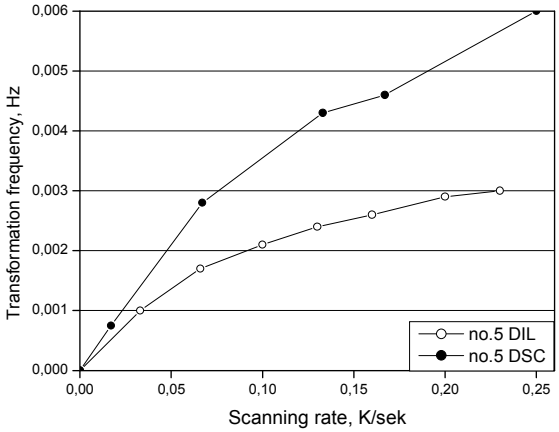

Fig. 6.4 b: A comparison of transformation frequencies measured dilatometrically (DIL) and calorimetrically (DSC) vs. scanning rate (sample 5)

6.2.2 Transformation with a single phase boundary

The own transformation velocity with stationary conditions was observed and directly measured during the transformation of the sample 1 under constant load (iso-stress conditions). The transformation begins during the very slow thermostatic cooling at the starting temperature $M_S = 12{,}1°C$ by nucleation a single martensite band (Fig. 6.5 a) on the one sample edge, its only one phase boundary moves at the holding after the transformation starting constantly environment temperature $T = M_S = 12{,}1°C$ (Isotherm transformation). In this way the whole sample transforms with the time completely into the martensite. This leads to change of sample length under constant load (Fig. 6.5 b), which has been recorded as a function of the temperature and the time.

The velocity of the phase boundary (the velocity of the band width increasing $\dot{\Lambda}$) was calculated from the velocity of sample length change ($\frac{d(\Delta l)}{dt}$) measured experimentally:

$$\dot{\Lambda} = \frac{d(\Delta L)}{\varepsilon_M dt} \approx 1{,}2 \times 10^{-4} \frac{m}{s}, \tag{6.11}$$

whereby $\varepsilon_M \approx 0{,}082$ is the martensitic deformation inside of the martensite band determined experimentally by the band width increasing (Λ) measured light-microscopically and the sample length change (ΔL) recorded simultaneously as following:

$$\varepsilon_M = \frac{\Delta L}{\Lambda} \approx 0{,}082\,. \tag{6.12}$$

This deformation remains constant during the progressive movement of the phase boundary. A thermocouple placed in the centre of the sample on its surface shows the increasing of temperature about 0,5°C during the phase boundary passing under this place due to the spending of the latent transformation heat (Table 4.2) on the moving phase boundary (exothermal direct transformation).

The single phase boundary reaches during the just as very slow heating its indifferent equilibrium at the temperature $T_0 = 12{,}7°C$, wherein it is slowly creeping there and back (Fig. 6.5 b). The iso-stress reverse transformation starts as the shrinking of the martensite band by the return motion of the same single phase boundary at the far slow heating up to the temperature $A_S = 13{,}9°C$ and is going on isothermally (after the starting of the reverse transformation the en-

vironment temperature was hold constant). The velocity of the phase boundary motion during the reverse transformation is somewhat smaller than $1{,}2\times10^{-4}\,\frac{m}{s}$ (6.11).

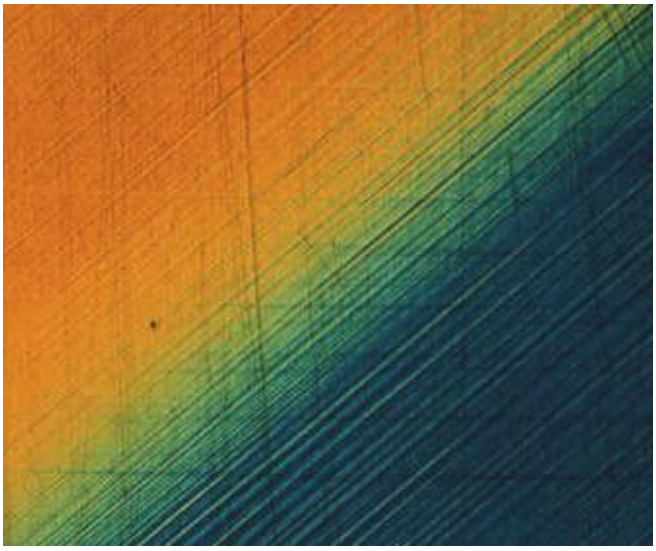

Fig. 6.5 a: A single phase boundary in the sample 1 between the growing martensite band (yellow) and the austenite (blue). Light microscopy, x50)

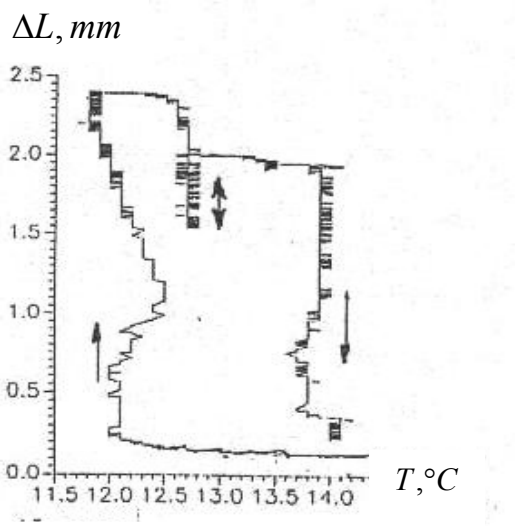

Fig. 6.5 b: Length ant temperature change of sample 1 during the isostress and isotherm direct and reverse stationary transformations due to moving of the single phase boundary

This velocity v is calculated direct from the experimentally recorded curves $\Delta L(t)$ as the slope $v=\frac{\Delta L(t)}{\Delta t}=const$ of their linear sections. Between these linear sections the phase boundary is braked again and again by defects or stopped for some time, so that the average velocity of the boundary is still smaller indeed. The full time needed for the direct and reverse migration of the phase boundary through the sample with the length of 25 *mm* and directly measured amounts to nearly 1000 *sec*, so that the frequency a one actuators of this length (independent of its cross section) in this case of zero scanning rate ($\dot{T}=0$) would amount to only about 0.001 *Hz*. In consideration of results represented in Fig. 6.4 a this means that the martensitic transformation in SMA's can be accelerated by the scanning rate increasing up to tenfold, but then a saturation takes place under one frequency limit.

Even in that ideal case in absence of elastic interaction with other martensite crystals and grain boundaries so small own velocity of the "thermo-elastic" (in this case rather not) martensitic transformation causes the inertia of the phase transformation in SMA's and their action frequency limiting. It connects with the breaking of phase boundaries by the own latent transformation heat as well as partially by their pinning through different defects..

6.2.3 Heat transfer in a one complete transformation cycle

In order to accomplish a complete transformation cycle, a SMA-actuator have to be once cooled down and once heated over the temperature interval $A_f \div M_f$ (with the considering its extension by not stationary conditions with the concrete scanning rate).

The heat balance in a complete transformation cycle at the heating of a SMA-actuator with the mass *m*, the entire heat radiation surface *A*, the electrical resistance *R* by the electric cur-

rent *I* and with its following conventional cooling in air with the temperature T_a contain the following terms:

$$\lambda A(T - T_a) = mc_p\left(A_f - T\right) + mT_0\Delta s^{AM} z \quad \text{for the adiabatic cooling and} \qquad (6.13\ a)$$

$$I^2 Rt = mc_p\left(M_f - T\right) - mT_0\Delta s^{MA}(1 - z) \quad \text{for the adiabatic heating,} \qquad (6.13\ b)$$

whereby λ is the convection coefficient, *T* is the current temperature of the SMA-actuator and c_P is the specific heat capacity of the SMA. It shouldn't be forgotten in this consideration, that the second terms (the latent transformation heat $Q^{AM,MA} = m \cdot q^{AM,MA} = m \cdot T_0 \cdot \Delta s^{AM,MA}$) in (6.13) normally have the same order of magnitude as the first terms (Joule's heat).

The heat transfer equations for the direct and the reverse transformations are to get by the time differentiating of the equations (6.13) with the consideration of the experimentally proven fact that the finish temperatures are dependent on the scanning rate and thus must be regarded as time variables::

$$\lambda A\dot{T} = mc_p(\dot{A}_f - \dot{T}) + mT_0\Delta s^{AM} \cdot \dot{z}^{AM} \qquad (6.14\ a)$$

$$I^2 R = mc_p(\dot{M}_f - \dot{T}) + mT_0\Delta s^{MA} \cdot \dot{z}^{MA} \qquad (6.14\ b)$$

It follows from (6.14) as the first that the transformation rate $\dot{z}$ is the smaller, the larger is the specific latent transformation heat:

$$\dot{z}^{AM} = \frac{\dot{T}\left(\lambda A + mc_p\right) - mc_p\dot{A}_f}{q^{AM}} \quad \text{und} \qquad (6.15\ a)$$

$$\dot{z}^{MA} = \frac{I^2 R + mc_p(\dot{T} - \dot{M}_f)}{q^{MA}}. \qquad (6.15\ b)$$

The conditions (6.15) show secondly that it is no frequency increasing by the unlimited increasing of the amperage or cooling rate $\dot{T}$ possible, because the extension rate of the transformation temperature range rises too and acts against in such a wax that the transformation rate $\dot{z}$ remains very limited and the transformation does not let accelerate itself so easily.

Conclusion

The theoretical and experimental results presented in this work prove thus clearly that dilatometry is very suitable as method for the investigation of martensitic transformations in SMA's despite hardly existing variation in volume namely not only in order to determine the transformation temperatures and thermal hysteresis, but also to investigate some physical processes accompanying the transformation.

Dilatation measurements allow to distinguish two parallel running and crystalographically different martensitic transformations, which do not differ thermodynamically and thus are not to differ calorimetrically.

With the help of dilatometry accommodation processes can be investigated, and accommodation degree can be calculated from dilatometric results.

Hysteresis loops determined dilatometrically yield all usual data about the transformation temperatures and the width of thermal hysteresis. The expansion coefficients in two-phase temperature ranges, calculated from the hysteresis loop are quantitative characteristics of transformation kinetics and their ratio describes qualitatively the symmetry of this hysteresis loop.

The purely dilatometric effects like the invare behaviour of samples in the martensitic state are to be determined anyway only with this method and were mostly determined in some investigated SMA's.

The expansion of hysteresis loops and of transformation temperature ranges determined dilatometrically at rising scanning rates is still larger because of larger masses of dilatometric samples than that of determined calorimetrically ones. Physical limiting of the action frequency of SMA-actuators is caused by the small own velocity of phase boundaries during the transformation due to their breaking by the latent transformation heat and partly due to their pinning by various structural defects.

Literature:

1. I. W. Hunter and S. Lafontane. A comparison of muscle with artificial actuators. – IEEE 1992,178-185
2. C. Schmidt, K. Neuking und G. Eggeler. Funktional fatique of shape memory polymers. – Advanced Eng. Materials 10(2008)922-927.
3. R. G. S. Barsoum. Active materials and adaptive structures. – Smart Mater. Struct., 6(1997)117
4. V. Pasler at al.. 3D-XY critical fluctuations of the thermal expansivity in detwinned $YBa_2Cu_3O_{7-\delta}$ single crystals near optimal doping. – Phys. Rew. Lett. 81(1998)1094
5. P. Nagel. Thermodynamik und Kinetik der Sauerstoffordnung in $YBa_2Cu_3O_x$. – Dissertation, Forschungszentrum Karlsruhe GmbH, Karlsruhe, 2001
6. V. Prieb, V., Structure and properties of *NiTi* alloys after treatment by the powerful electronic impulses with nanosecond length. In the Proc. of the "ESOMAT`91", France. – J. de Phys. IV 11(1991)317
7. V. Prieb. Formation of non-equilibrium structures in metal alloys under high intensity electron beams and metrology of these beams with a help of memory alloy targets. – Proc. of the 2nd Int. Conf. „Radiation-thermal defects and Processes in inorganic materials", Tomsk, 2000, p.10 (http://materialforschungsservice-dr-prieb.de/Bestrahlung.pdf)
8. Y. Matsuzaki. Smart structures research in Japan. – Smart Mater. Struct. 6(1997)R1
9. J. Van-Humbeck and Y. Liu. Shape memory alloys as damping materials. – Mat. Sci. Forum (SMM'99) 327(2000)331
10. J.J. Wang et al. Microstructure and thermal expansion properties of invar-type Cu-Zn-Al shape memory alloys. – J. of Electronic Mater. 10(2004)3776
11. M. Boabdallah and G. Gitzeron. Caracterisation des changements de phase developpes dans un alliage AMF du type Cu-Al-Ni, par dilatometrie de trempe et microcalorimetrie differentielle. – The Eur. Phys. J. – AP 1(1998)163
12. J. Uchil, K.K. Mahesh and K.G. Kumara. Dilatometric study of martensitic transformation in NiTiCu and NiTi shape memory alloys. – J. of Mater. Sci. 36(2001)5823
13. I. Szurman, M. Kursa, Z. Jedlicka. Transformation temperatures of Ni-Ti based alloys measured by resistometric and thermo-dilatometric methods. – Acta Met. Slovaca 12[2006]411
14. "ACTUATOR'98" – Proc. of 6th Int. Conf. on New Actuators, Bremen 1998
15. V. Prieb, and V. Wolff. The limiting of the response time of shape memory alloy actuators by transformation rate. – Proc. of the Int. Conf. on the SMA-Applications, Kiew, 2000 (http://www.materialforschungsservice-dr-prieb.de/ratelimit.pdf)
16. Z. Dong et al. A novel Fe-Mn-Si shape memory alloy with improved shape recovery properties by VC precipitation.a – Advanced Eng. Mater. 11(2009)40

17. V. Prieb. The mechanical behaviour of a Cu-Zn-Al shape memory alloy with a single-interface transformation. – Proc. of “ACTUATOR´94”, 15-17 June 1994, Bremen, Germany, p.p. 365-370 (http://www.materialforschungsservice-dr-prieb.de/ACTUATOR94.pdf)

18. K. Madangopal, J.B. Singh and S. Banerjee. The Nature of Self-Accommodation in Ni-Ti Shape Memory Alloys. – Scr. Metal., 29(1993)725

19. S. Fu, Y. Huo and I. Müller. Thermodynamics of pseudoelasticity - an analytical approach. – Acta Mech. 99(1993)1

20. V. Prieb and V. Wolff. The hysteresis loop interior of the thermoelastic martensitic transformation. – Report on the Int. Conf. on the Martensitic Transformation „KUMICOM-99“, Moscow, 1999 (http://www.materialforschungsservice-dr-prieb.de/Hystereseinnere.pdf)

21. W.I. Buehler, J.V. Giefrich , R.C. Willy. – J. Appl. Phys. 34(1963)1475

22. P. Roumagnac et al. Mechanical behaviour and deformation mechanisms of Ni-Ti shape memory alloys in tension. – The Europ. Phys. J. – Appl. Phys. 10(2000)109.

23. V. Prieb and H. Steckmann. Thermoelasticity and hysteresis of martensitic transformation in shape memory alloys. I. Hysteresis of the stress-free thermal transformation. – Tech. Phys., 41(1996)1132 (http://www.materialforschungsservice-dr-prieb.de/Thermohysterese.pdf)

24. V. Prieb, H. Steckmann and V. Wolff. Thermodynamic parameters of the martensitic transformation of NiTi-X shape memory alloys. – Mater. Sci. Trans. 6(2000)12 (http://www.materialforschungsservice-dr-prieb.de/ThermoParameter.pdf)

25. V.Prieb, V. Udovenko et al. Martensitic transformation in antiferromagnetic alloys of NiMn intermetallic compound. – Z. Metallkd. 86(1995)345

26. V. Prieb et al. Influence of the structure and orientation of the parent phase on the hysteresis of single-crystal shape memory alloys. In the Proc. of the Int. Conf. on the Mart. Transf. „ICOMAT ´95“ – J. de Phys. 5(1995)C8-913

27. V. Prieb and H. Steckmann. Pseudo-Plastic Behaviour of Single-Crystals of Cu-Base Memory Alloys. In the Proc. of the Int. Conf. on the Mart. Transf. „ICOMAT ´95“ – J. de Phys. 5(1995)C8-907

28. V. Prieb et al. Influence of texture on the shape memory effect in TiNi.. – Mater. Sci. Trans. (Rus.) 9(1979)62

29. Ken Ho, P. Jardine, G.P. Carman, and C.J. Kim. Modeling and Measuring the Responce Times of Thin Film TiNi. – SPIE 3040(1997)10

30. P.L. Potapov. Thermoelectric triggering of phase transformations in Ni-Ti shape memory alloy. – Mater. Sci. and Eng. B52(1998)195

Dr. Viktor Eduard Prieb - physicist, poet, writer, journalist, translator - was born in 1951 as "Soviet citizens of german nationality" (official formulation of NKVD / KGB for the banishment and deportation reason of Germans from Russia) in a special German settlement near Novosibirsk in Siberia under commandery supervision.

Since 1990 lives with his family as "German citizens of german nationality" in Germany, since 1993 in Berlin.

In years 1968 - 1975 studied physics and computer science at the Novosibirsk and Tomsk State University, Department of - Solid State Physics, conclusion – physicist-mathematician, Thesis: "*Influence of texture on the shape memory effect in TiNi*". In 1983 graduated in the Tomsk University to Dr. rer. nat. Topic of the thesis: "*Magneto-structural transformations and shape memory effects in Fe-Mn and Fe-Mn-C alloys*". For nearly 40 years researched intensively in the field "Memory alloys".

Other research fields: "*Investigation of dielectrics and epitaxial semiconductor structures*" (1983 - 1985), "*Surface treatment of metallic alloys by their irradiation with strong electron pulses in the nanosecond length range*" (1985 - 1991), "*Ultrasonic treatment and welding of metal parts*" (1998 - 2002) .
In 1992 participated in the training course for software developers at Fa "Siemens-Nixdorf" in Essen, NRW, Germany.

In years 1993 - 1995 worked as a research assistant at the TU-Berlin on about "*Growing of single crystals of Cu-based shape memory alloys and investigation of their thermoelasticity and thermal hysteresis*".

In years 1995 - 2002 was a founder and scientific-technical director of the company "1st Memory Alloys GmbH" (*research of shape memory alloys and development of their applications*).

Since 2002 carries out materials research service, genealogy, sociology, political science research and intensive bilingual literary activity (*poetry, prose, journalism, poetic translations and their analysis*).

Siberian “*quenching*” saves from fatigue, and Siberian "*awareness*" over many years saves before falling asleep of curiosity and interest.